

In presenting the dissertation as a partial fulfillment of the requirements for an advanced degree from the Georgia Institute of Technology, I agree that the Library of the Institute shall make it available for inspection and circulation in accordance with its regulations governing materials of this type. I agree that permission to copy from, or to publish from, this dissertation may be granted by the professor under whose direction it was written, or, in his absence, by the Dean of the Graduate Division when such copying or publication is solely for scholarly purposes and does not involve potential financial gain. It is understood that any copying from, or publication of, this dissertation which involves potential financial gain will not be allowed without written permission.

7/25/68

THE INFLUENCE OF FABRICATION SCHEDULES ON
THE MECHANICAL BEHAVIOR OF A-441 STEEL

A THESIS

Presented to

The Faculty of the Graduate Division

by

Manuel Rafael Pereyra

In Partial Fulfillment

of the Requirements for the Degree

Master of Science in Mechanical Engineering

Georgia Institute of Technology

June, 1970

THE INFLUENCE OF FABRICATION SCHEDULES ON
THE MECHANICAL BEHAVIOR OF A-441 STEEL

Approved:

/

Chairman

0

Date approved by Chairman: 6/5/76

ACKNOWLEDGMENTS

Many individuals and organizations rendered assistance to the accomplishing of this thesis, and their considerable help is greatly appreciated. The Fundacion Creole of the Creole Petroleum Corporation made funding available for the entire graduate study program. The experimental fabrication program would have been impossible without the cooperation of the Republic Steel Corporation; particular thanks are due Dr. A. B. Blocksidge, Jr., Assistant Director of Research, and Dr. C. B. Griffith, Chief, Metallurgical Development Section.

Dr. W. R. Clough initially suggested the program, implemented its progress, and worked closely with me. Drs. J. M. Bradford and R. F. Hochman gave help and advice on several occasions; work at the metallograph in the School of Chemical Engineering was possible only because of Dr. Hochman's assistance. Messrs. R. G. Grim, B. L. Wallace, H. J. Carr, L. A. Cavalli, and J. W. Davis gave advice and assistance when specimens were being prepared in the machine shop. The interest and help of Dr. E. E. Underwood, Associate Director, Material Science Research Division, Lockheed-Georgia Research Laboratories, was of importance. It was a pleasure to work closely with Mr. Y. M. Ebadi who was simultaneously completing a related thesis.

The author would like to dedicate this thesis to his parents for their concern, love, and continued encouragement in the pursuance of his education.

TABLE OF CONTENTS

	Page
ACKNOWLEDGMENTS	ii
LIST OF TABLES	iv
LIST OF FIGURES	v
SUMMARY	vii
Chapter	
I. INTRODUCTION	1
Definition of the Problem	
High Strength, Low Alloy Steels	
Property, Microstructure, and Composition Interrelations	
The Thermomechanical Treatment of Steel	
II. MATERIAL, FABRICATION, AND SPECIMEN PREPARATION	27
A-441 Steel	
The Thermomechanical Treatment Project	
Preparation of Test Specimens	
III. EXPERIMENTAL PROCEDURES	37
Tensile Tests	
Charpy Impact Tests	
Hardness Tests	
Metallographic Analyses	
IV. RESULTS	48
Mechanical Properties	
Metallographic Analyses	
V. CONCLUSIONS AND DISCUSSION	64
"Hot Work" Code Designation	
"Cold Work-Hot Work" Code Designation	
VI. RECOMMENDATIONS	92
BIBLIOGRAPHY	93

LIST OF TABLES

Table		Page
1.	Code of Designation of Fabrication Samples	31
2.	Tensile Test Results Related to Yielding, Hot Work Samples	50
3.	Tensile Test Results Related to Yielding, Cold Work-Hot Work Samples	51
4.	Tensile Test Results Related to Necking, Hot Work Samples	52
5.	Tensile Test Results Related to Necking, Cold Work-Hot Work Samples	53
6.	Tensile Test Results Related to Fracture, Hot Work Samples	54
7.	Tensile Test Results Related to Fracture, Cold Work-Hot Work Samples	55
8.	Charpy Test Results, Hot Work Samples	56
9.	Charpy Test Results, Cold Work-Hot Work Samples	58
10.	V-Notch Charpy Transition Temperature	60
11.	Hardness Test Results, Hot Work Samples	61
12.	Hardness Test Results, Cold Work-Hot Work Samples	61
13.	Optical Metallographic Results, Hot Work Samples	62
14.	Optical Metallographic Results, Cold Work- Hot Work Samples	63

LIST OF FIGURES

Figure		Page
1.	Location of Test Samples Relative to Fabricated Plate	35
2.	Test Specimen Dimensions	36
3.	Yield Strength and Ultimate Tensile Strength as Functions of Fabrication Temperature, Hot Work Longitudinal Specimens	68
4.	Applicability of Hall-Petch Equation for High Temperature Fabricated A-441, Hot Work Longitudinal Specimens	69
5.	Yield Strength and Ultimate Tensile Strength as Functions of Fabrication Temperature, Hot Work Transverse Specimens	70
6.	Strain Hardening Exponent as a Function of Fabrication Temperature, Hot Work Longitudinal Specimens	71
7.	Strength Coefficient as a Function of Fabrication Temperature, Hot Work Longitudinal Specimens	72
8.	Strength Coefficient as a Function of Fabrication Temperature, Hot Work Transverse Specimens	73
9.	Percent Elongation as a Function of Fabrication Temperature, Hot Work Transverse Specimens	74
10.	Percent Elongation as a Function of Fabrication Temperature, Hot Work Longitudinal Specimens	75
11.	V-Notch Transition Temperature as a Function of Fabrication Temperature, Hot Work Specimens	76
12.	Ferrite Orientation Factor as a Function of Fabrication Temperature, Hot Work Specimens	77
13.	Photomicrographs, Hot Work Samples:	78
	(a) Specimen O	
	(b) Specimen P	
	(c) Specimen R	
	(d) Specimen T	

LIST OF FIGURES (Continued)

Figure		Page
14.	Yield Strength and Ultimate Tensile Strength as Functions of Fabrication Temperature, Cold Work-Hot Work Longitudinal Specimens	82
15.	Applicability of Hall-Petch Equation for High Temperature Fabricated A-441, Cold Work-Hot Work Longitudinal Specimens	83
16.	Yield Strength and Ultimate Tensile Strength as Functions of Fabrication Temperature, Cold Work-Hot Work Transverse Specimens	84
17.	Strain Hardening Exponent as a Function of Fabrication Temperature, Cold Work-Hot Work Longitudinal Specimens	85
18.	Strength Coefficient as a Function of Fabrication Temperature, Cold Work-Hot Work Longitudinal Specimens	86
19.	Strength Coefficient as a Function of Fabrication Temperature, Cold Work-Hot Work Transverse Specimens	87
20.	Percent Elongation as a Function of Fabrication Temperature, Cold Work-Hot Work Specimens	88
21.	Percent Elongation as a Function of Fabrication Temperature, Cold Work-Hot Work Transverse Specimens	89
22.	V-Notch Transition Temperature as a Function of Fabrication Temperature, Cold Work-Hot Work Specimens	90
23.	Ferrite Orientation Factor as a Function of Fabrication Temperature, Cold Work-Hot Work Specimens	91

SUMMARY

An objective of this thesis was to determine the possibilities of improving the mechanical properties of production rolled A-441 steel plate by applications of several thermomechanical treatments. A-441, a triple alloy addition high strength low alloy steel, was selected as the experimental material to be investigated since no work involving controlled rolling has been reported for this alloy and since the triple alloy additions might be expected to produce unusual responses. The experimental fabrication program involved rolling samples of production mill processed and initially cold worked A-441 plate at temperatures selected to span pertinent portions of the iron - iron carbide metastable binary equilibrium phase diagram.

A unique combination of properties resulted when fabrication was accomplished just above the A_3 line. Austenite would be expected to be strain hardened with resulting improvements in room temperature properties after metallurgical transformations. Processing at the indicated temperature resulted in unusually low Charpy V-notch ductile-brittle transition temperatures and improved values of yield strength, ultimate tensile strength, and ductility, as compared with values obtained from specimens prepared from mill processed A-441. It was concluded that HTMT was an unusually effective thermomechanical treatment for A-441 and PTMT was not.

Fabrication at temperatures above 1400°F resulted in property variations controlled by ferrite grain size, and the well known

Hall-Petch relationship was applicable. Fabrication below 1400°F introduced cold work effects, possibly complicated by strain aging, and resulted in partially oriented ferrite grain structures. Fabrication at 1400°F, just above the A_3 line, resulted in a unique microstructure involving small and equiaxed ferrite grains and small and well dispersed patches of pearlite. The microstructure so obtained is very desirable.

are "hot worked." For the steels considered, such a temperature range is well into the single phase austenitic region. Steels of a given composition or designation produced by a given combination of processes will then be represented by a given set of mechanical properties which will show but little variation of properties from heat to heat, so the design engineer then has available a "standard" set of properties for each structural steel.

The problem with which this thesis is concerned was to experimentally determine if there is a preferable fabrication temperature or range of temperatures to give an optimum combination of mechanical properties, instead of the "standard" properties produced by common hot working procedures as mentioned in the last paragraph.

The properties to be considered in the thesis included yield strength, ultimate tensile strength, uniform elongation, percent reduction of area, percent elongation, strain hardening exponent, strength coefficient, all as determined from room temperature tensile tests, and ductile-brittle transition temperatures as established by V-notch Charpy testing. Tensile and Charpy characteristics were to be determined for each sample involved in an experimental fabrication program, and the effects of changes of fabrication variables on microstructures were to be determined by utilization of available means.

It was decided that the steel to be studied would be one of the HSLA compositions. A triple low alloy grade, designated by the producer as Republic A-441, was selected: this steel contains low level alloy additions of manganese, vanadium, and copper. Other structural steels, including one single low alloy grade (X-52) and one double low alloy

grade (X-60), were simultaneously being investigated in other related research programs.

A most important part of the thesis involved an experimental fabrication program that could not be accomplished in Georgia Institute of Technology facilities; the fabrication program was made possible by the extensive cooperation of acknowledged personnel of the Republic Steel Research Center in Cleveland, Ohio. It was desired that Republic A-441 in two different initial conditions (mill finished and cold worked) be fabricated at several temperatures within the single phase austenitic region (above the A_3 line), at temperatures within the critical region (two phase austenite-ferrite range, between the A_1 and A_3 lines), and at several temperatures within the two phase ferrite-cementite range, below the eutectoid temperature. The specific temperatures and reductions to be used for experimental fabrication were specified by the author and his advisor, on the basis of experience and theory, but had to be compatible with the capabilities of the Republic Steel research fabrication facilities.

High Strength, Low Alloy Steels

General Considerations

A compilation of commercially available HSLA steels, both by composition and by manufacturer, has been made by the American Society for Metals [1]. In this compilation the HSLA steels are classified into three groups. The first is referred to as the "columbium or vanadium" group, and a characteristic is columbium or vanadium additions in excess of 0.01 w/o; another characteristic is relatively high manganese content, in the range from 0.7 to 1.7 w/o depending on the specific steel being

considered, which is somewhat in excess of the manganese content (0.3 to 0.5 w/o) of plain carbon steels of the same carbon content. The second group, "manganese and manganese-copper HSLA steels," conforms to ASTM A440 and SAE 950C. Composition ranges include 0.19 - 0.28 w/o C, 1.10 - 1.60 w/o Mn, and a minimum of 0.2 w/o Cu. The third classification of HSLA steels is referred to as the "manganese-vanadium-copper group," and a representative analysis includes 0.22 w/o Cu, 1.25 w/o Mn, 0.3 w/o Si, 0.20 w/o Cu, and 0.02 w/o V. The steel selected for study in this thesis falls within this third grouping.

With the commercial introduction of HSLA steels it has been recognized that the properties of hot rolled carbon steels are considerably modified or altered by those small alloy additions which promote [2,3,4]*:

1. Increased hardenability to form finer and therefore stronger ferritic-pearlitic structures. In this sense hardenability does not refer to martensite or bainite formation.
2. Increased ferrite strength.
3. Improved corrosion resistance.
4. A precipitation hardening capability.

The presence in steel of common alloying elements such as carbon, nitrogen, manganese, silicon, nickel, chromium, molybdenum, copper, columbium, and vanadium in solid solution in the austenite phase results in a significant increase in hardenability; note that the term "hardenability" as here used refers to the general phenomena of retardation of

*

Numbers in [] refer to references listed in the Bibliography.

the transformation of austenite. When this retardation occurs during continuous cooling the formation temperature of ferrite is thus lowered and there is then a decrease of ferrite grain size; the proportion or volume percent of ferrite is also decreased, resulting in an increase of pearlite. Most alloying elements also strengthen ferrite steels by substitutional solid solution hardening mechanisms. Phosphorus is a most potent solution strengthening addition and is used judiciously in several steels. Copper is also widely used as a strengthening addition, and manganese and nickel additions improve toughness in addition to raising strength.

Specific alloy additions to HSLA steels are also able to noticeably improve atmospheric corrosion resistance. Chromium, copper, phosphorus, silicon, and nickel are considered to be the most beneficial additions [5]. As little as 0.2 w/o Cu is sufficient to double the atmospheric corrosion resistance of carbon steels, but the increasing of Cu concentration beyond this level is less effective. Thus, in addition to higher strength levels, several hot rolled HSLA steels have sufficiently improved corrosion resistance to noticeably prolong paint life, and the steels are actually often used in the unpainted condition in many structures.

It is generally true that the levels of alloy additions that can be made to improve the strength of HSLA steels are limited by weldability considerations. Since structural steels are often welded, there has been a concentrated search for those alloy additions which would be particularly potent strengtheners at low concentration levels, and great attention has been given to the precipitation hardening additives,

particularly columbium and vanadium.

Columbium has been found to be a very useful strengthening agent for the very practical reason that it can be added to the large number of semikilled steels that provide maximum columbium yield from the ingot: the affinity of columbium for oxygen is sufficiently low that about 90 w/o can be recovered from ladle additions to killed or semikilled steels. However, the recovery in rimmed steels is quite low, from 15 to 50 w/o, and with increasing additions the recovery decreases so sharply that it is indeed difficult to reach a level of 0.02 w/o Cb in rimmed steels [6] .

Several major modifications in the behavior of steels are caused by alloying at low levels with columbium, since even at low concentration levels there is the possibility of compound formation with resulting hardening effects. Columbium carbide and nitride have complete solid solubility so that the compound found in commercial columbium containing HSLA steels is referred to as a carbonitride. It has been shown [7,8] that with a steel containing 0.2 w/o C, 0.1 w/o N, and 0.03 w/o Cb that a temperature of 2100°F is necessary to place the columbium carbonitrides in solid solution; normal soaking pit practice, at or above 2300°F, should insure solution of the columbium carbonitrides. With HSLA steels it appears to be well documented that there are four principle effects introduced by the presence of columbium.

One important effect of columbium additions is that the recrystallization temperature of austenite is raised, and the rate of austenite recrystallization is retarded. Effects on the recrystallization kinetics are due to the fact that columbium carbonitride can be formed in

with columbium or vanadium.

The technical literature dealing with HSLA steels and the various columbium and vanadium effects in steel has become extensive and voluminous. An excellent review article which traces the development of HSLA structural steels has recently been published by Irving [16], and the entire volume which contains this paper has a wealth of technical information regarding applications of HSLA steels and the commercial production and fabrication procedures utilized with these steels. In addition to the papers which were previously mentioned, the research papers of Stephenson, Karchner, and Stark [17] dealing with strengthening mechanisms in Mn-V-N steels and of W. B. Morrison [18] dealing with the influence of small columbium additions on the properties of various carbon-manganese containing steels are regarded as technical milestones.

Republic A-441

As previously mentioned, Republic A-441 is a triple low alloy grade of HSLA steel containing manganese, vanadium, and copper, and it is considered to have outstanding features as regards a combination of strength and toughness. Advertising literature [19] values of mechanical properties include 50,000 psi yield point minimum, 70,000 psi ultimate tensile strength minimum, and 22% tensile elongation in a two inch gage length. The 15 ft. lb. Charpy V-notch transition temperature is given as 0°F. Welding characteristics are considered to be excellent by the usual methods such as manual, arc, semi- and full automatic, resistance, and gas welding. Republic A-441 meets or exceeds specifications given by ASTM A441 and A242 for plates, structurals, and bars, and ASTM A374 and A375 for sheet. The steel is widely used in

bridges, buildings, and construction equipment, and is available as hot rolled sheet, hot dip galvanized sheet, hot rolled strip, hot rolled plate, hot rolled bar and bar shapes, and hot rolled structural shapes. Tensile strengths and yield points will be reduced by 5,000 psi by annealing or normalizing the hot rolled sheet.

Property, Microstructure, and Composition Interrelations

Ferrite Grain Size

It is now an established fact that variations of grain size will greatly influence the values of many mechanical properties, for a given alloy, if grain size is the only variable which is altered from sample to sample. For example, room temperature evaluations have shown that hardness, yield strength, ultimate tensile strength, fatigue strength, and impact resistance all increase with decreasing grain size. The effect of grain size is no doubt a maximum when dealing with those characteristics which are of importance in the early stages of deformation in the plastic range, for it is at this stage of flow that grain boundary barriers to dislocation motion are most effective. Thus, it would be expected that yield strength would be more dependent on grain size than would ultimate tensile strength. For plastic deformation at relatively large strains the value of the flow stress would be chiefly controlled by complex dislocation interactions taking place within the grains, and then grain size would not be the controlling variable for mechanical properties.

A well respected and quite often utilized relationship between yield strength, σ_y , and a measure of grain size, as the grain diameter d , is one derived from considerations of basic dislocation theory by

Hall [21] and Petch [22]. The relationship is so well known and so well documented that it is commonly referred to as the Hall-Petch equation, which is as follows:

$$\sigma_y = \sigma_i + K_y d^{-\frac{1}{2}} \quad (1)$$

It is obvious that this relationship would result in linearity if the yield strength, σ_y , would be plotted as the ordinate against the reciprocal of square root grain diameter ($d^{-\frac{1}{2}}$) as the abscissa. The friction stress, σ_i , is that which opposes the motion of dislocations, while K_y is a measure of the extent to which dislocations are piled up at a barrier, as against a grain boundary. The strength coefficient, K_y , which has been found to be essentially independent of temperature, would be evaluated from the slope of the mentioned plot. The value of the intercept on the plot, σ_i , is a measure of the stress required to drive a dislocation against the resistance offered by impurities, precipitate particles, subgrain boundaries, the Peierls-Nabarro force, and other obstacles to dislocation motion. Composition, metallurgical condition, and temperature determine the value of the friction stress term. The Peierls-Nabarro force is also temperature dependent, and other resistances to the dislocation motion are influenced by both temperature and composition, thus indicating the necessity of applying Equation 1 only for a given metal with samples in identical condition except for grain size. The Hall-Petch relationship was initially proposed after considerations of the yield point behavior of low carbon steels, but it has now been applied to a very wide variety of steels and many nonferrous

alloys. It has been estimated in a recent article that the Hall-Petch equation has now been verified for over 60 cases. Of course, values of σ_i and of K_y vary from alloy to alloy, and from metallurgical condition to condition for a specific alloy.

Many of the alloy additions which are made to low carbon steels result in some solid solution strengthening of the ferrite and thereby raise values of the lattice friction stress σ_i . At the same time, these alloys may result in the austenite-ferrite transformation being altered to lower temperatures, thus producing a refinement in ferrite grain size. Both of the effects here mentioned will raise the yield strength of such steels as dictated by the Hall-Petch equation. When effects of the type mentioned in this paragraph are the only ones of importance for the steels being considered, quantitative metallographic procedures and multiple regression analyses done with computers have allowed the two simple metallurgical effects to be separated, and it is then possible to express the Hall-Petch relationship in terms of chemical composition, in the general form:

$$\sigma_y = C_1 + C_2 d^{-\frac{1}{2}} + \sum_{i=1}^N \alpha_i \quad (2)$$

α_i is the strength increase, in the units of psi for example, per weight percent of alloy in solid solution in the ferrite. The summation is taken over the N alloy additions which are in solution in the ferrite. Note that relationships of the form of Equations 1 and 2 take no account of cold work, aging, precipitation effects, or the other complicated metallurgical phenomena which may be expected to influence values of the friction stress σ_i : this fact cannot be overemphasized, and must

be kept in mind in the remaining portions of this thesis.

Pickering's group [23,24] at the United Steel Companies, Limited, of Great Britain accomplished the original work in the development of relationships as Equation 2. The analyses considered variables as grain size (ferrite) and volume fraction of pearlite and solution hardening effects and cooling transformation effects due to alloy additions such as manganese and silicon. The computer regression analyses were made over rather wide ranges of steel compositions common only to structural steels, and only considered the steels when in soft conditions as would result from normalizing. The result of the yield strength regression analysis was:

$$\sigma_y (\text{psi}) = 15,000 + 4,720(\text{w/o Mn}) + 12,150(\text{w/o Si}) + 507d^{-\frac{1}{2}} \quad (3)$$

The equation was not considered to be able to handle the effects introduced by those alloy additions which cause more complicated metallurgical phenomena, as precipitation hardening due to vanadium or columbium carbonitrides, cold work, or strain aging. Various modifications of Pickering's pioneer formulation have been developed since 1963, and in 1967 Jamieson and Thomas [25] published the following relationship developed on considerations involving only one steel fabricated by two different mill practices:

$$\sigma_y = 8,700 + 73,900(\text{w/o C}) + 12,200(\text{w/o Mn}) + 102,200 (\text{w/o V}) + 278d^{-\frac{1}{2}} \quad (4)$$

Duckworth and Baird [26] developed a formulation allowing σ_y calculation

for carbon steels in the usual mill hot worked condition, but the silicon contents of the considered steels was quite low, so there resulted:

$$\sigma_y = 11,872 + 3.189(w/o \text{ Mn}) + 573d^{-\frac{1}{2}} \quad (5)$$

Irvine [27] has developed the following minor modifications of the Pickering equation:

$$\sigma_y = 10,080 + 4,704(w/o \text{ Mn}) + 12,096(w/o \text{ Si}) + 51,520(w/o \text{ N}_f^{\frac{1}{2}}) + 502d^{-\frac{1}{2}} \quad (6)$$

The Irvine relationship is somewhat unique in that it separately accounts for the weight percent free nitrogen, N_f , in solution in the ferrite grains.

Some investigators believe that the effects of pearlite on yield strength values may be more important than simple reasoning would lead one to believe. Korchynsky [28] and his associates at the Graham Research Laboratories of the Jones and Laughlin Steel Corporation, Pittsburgh, Pennsylvania, gave further modifications to Pickering's formulation by considering the volume fraction (v/o) of pearlite present in microstructures, obtaining:

$$\sigma_y = 13,000 + 3,500(w/o \text{ Mn}) + 9,000(w/o \text{ Si}) + 4,000(w/o \text{ Ni}) + 99(v/o \text{ pearlite}) + 591d^{-\frac{1}{2}} \quad (7)$$

The influence of ferrite grain size and volume fraction of pearlite on the lower yield strength and Luders strain of carbon steel has been

influence σ_i values for steels, and changes of value of σ_i will be reflected in changes of value of several mechanical properties. Numerous investigators, including Pickering and Gladman [23], have considered that for the case of plain carbon steels with carbon contents below 0.2 w/o, the value of σ_y is independent of the volume fraction of pearlite in the steel, allowing the development of relationships such as Equations 3, 4, 5, and 6. These research workers have reasoned that although the pearlite patches are comparatively hard, as opposed to ferrite grains, that they are so widely dispersed in the ferrite matrix that the ferrite can deform around them with but little difficulty. This reasoning is disputed, however, by relationships such as Equation 7. It has been found [30] that pearlite formation can influence ferrite grain size; ferrite grain size generally decreases with increasing pearlite volume fraction because the formation of pearlite patches during the austenite decomposition transformation interferes with ferrite grain growth. After plastic flow has been well initiated in the tensile test and after the cross-sectional area of the specimen is thus reduced, the pearlite patches are closer together and then can exert possibly significant plastic constraint factors upon further deformation of the ferrite; a result will be an increase of strain hardening rate, and thus an expected result would be that the ultimate tensile strength of annealed carbon steels would be increased by the presence of pearlite. Equations 8 and 9 verify these postulations.

The yield strength of steel is increased by increasing carbon concentration [31]. This increase takes place because increasing carbon lowers the austenite-ferrite transformation temperature and

consequently causes a reduction in ferrite grain size. The friction stress σ_i also increases with increasing carbon content [33]. Both effects are more pronounced as cooling rates from the austenitic region are increased because the carbon then precipitates at lower temperatures and the grain refining action and precipitation hardening effects are increased.

Increasing carbon content also increases the V-notch Charpy ductile-brittle transition temperature [32]. The greatest effect is due to the increased size and number of carbides that form at ferrite grain boundaries, for a given cooling rate after austenitizing; the grain carbides act as excellent brittle crack starters. A smaller effect is due to the fact that increasing carbon increases the value of σ_i directly.

The V-notch Charpy characteristics of quenched low carbon steels are generally superior to those of normalized or even annealed low carbon steels since the fast cooling rate prevents the formation of grain boundary cementite and also refines ferrite grain size. The ferrite grain size of normalized steel can be diminished, however, by lowering the normalizing temperature. The ductile-brittle Charpy transition temperature of a low carbon steel has been lowered by 125°F by reducing the normalizing temperature from 2200 to 1650°F [34].

Many grades of structural steel are utilized for engineering applications when in the hot rolled condition. Rolling to a lower than normal finishing temperature at the hot mill can lower the impact transition temperature [35,36,37], probably due to the increase of cooling rate and the correspondingly reduced ferrite grain size. Heat transfer considerations dictate that under equal circumstances thick plates cool

more slowly than thin plates, and the thick plates will thus have a larger ferrite grain size and higher ductile-brittle transition temperatures after identical thermomechanical treatments [38]. Post rolling normalizing treatments are sometimes given directly after hot rolling, to improve the properties of rolled plate by the just described mechanisms [39].

Deformation accomplished in the plastic region will elevate friction stress values of an alloy by strain hardening, and it is well known that the strengthening effects may be unusually large; it is not uncommon for the yield strength (flow stress) of steels to be doubled, tripled, or further increased by cold work. Correspondingly, the Charpy ductile-brittle transition temperature is also raised by cold work: an increase of transition temperature of about 4.5°F has been found to correspond to a 1,000 psi increase in σ_i promoted by previous 2% plastic strain [40].

There are other, indirect, effects which may be introduced by plastic deformation and cold work, since subsequent strain aging can also produce increases in σ_i values. The actual magnitudes of the friction stress increases resulting from strain aging will depend on the composition of the steel, the amount of previous cold work and the temperature at which it was accomplished, aging time, and aging temperature. Strain aging alterations of friction stress values are believed to result [41] from dispersion hardening effects brought about by the precipitation of iron nitride from solid solution. The return of the yield point drop on complete aging is thought to result from the pinning of dislocations by free nitrogen atoms, as has been postulated in several yield theories. The increase of friction stress σ_i due to strain aging

is capable of promoting strain aging embrittlement [42,43,44], and there is an increase of Charpy ductile-brittle transition temperature of about 3.6°F per 1,000 psi increase in σ_y due to such aging. Alloy additions to steel, as manganese, aluminum, and vanadium, lower the tendencies for strain age embrittlement, the former by retarding the precipitation of nitrides and the later two by gettering the nitrogen in the form of vanadium carbides or nitrides during normalizing or hot rolling. Silicon is also beneficial in this respect since it is an effective deoxidizer and thus leaves aluminum free to getter the nitrogen.

The greatest influence on friction stress σ_i values are associated with strain hardening and possible subsequent aging. In regard to strain hardening, the common engineering tensile stress-strain curve is really not suitable for describing the plastic behavior and work hardening characteristics of metals and alloys. Superior descriptions of work hardening are obtained when the tensile true-stress-true-strain curve is considered. It is often found that the true-stress-true-strain behavior in tension can be described by a formulation of the type:

$$\bar{\sigma} = K \bar{\epsilon}^n \quad (14)$$

Thus, there is implied a linear relationship between $\log \bar{\sigma}$ and $\log \bar{\epsilon}$, with the value of the slope of such a plot (when $\log \bar{\sigma}$ is plotted as the ordinate) being the value of the strain hardening exponent n , and the intercept being the value of true stress at a true strain value of one, the latter being designated by K and being known as the strength coefficient. If a material is found to obey the relationship given by Equation 14, Considere's constructions [52] will then show that it is

necessary for the true strain at the instant of necking to have a value equal to that of n . Thus, the strain hardening exponent is a measure of the rate of work hardening of the material being considered. A low slope value for the $\log \bar{\sigma} - \log \bar{\epsilon}$ plot indicates a low value of work hardening (change of flow stress with change of plastic deformation), and a low value of true elongation before necking commences. A high slope value corresponds to rapid work hardening. Many of the experimentally determined plots of $\log \bar{\sigma}$ against $\log \bar{\epsilon}$ for low alloy steels do not show actual linearity in the plastic range, and a number of modifications of Equation 14 have been proposed. A new relationship proposed by Gladman, Holmes, and Pickering [45] has been found to give excellent agreement with much experimental data obtained in tension with low carbon steel specimens:

$$\bar{\sigma} = a + b \ln \bar{\epsilon} + c \bar{\epsilon} \quad (15)$$

The Thermomechanical Treatment of Steel

General

The possibility of accomplishing hardening or strengthening, by pertinent metallurgical mechanisms, simultaneous with fabrication at the hot mill, or immediately following hot mill fabrication, is a matter that has received considerable research and development attention within the last several years. Some of the development experience has been reduced to commercial practice and is now utilized in the steel industry in this country, Great Britain, and the Soviet Union. Some of the procedures which have been developed have no applicability to this

thesis, but others do.

Controlled Cooling

The combination of accelerated cooling immediately after leaving the hot mill and control of coiling temperatures has received attention when dealing with relatively thin strip products. The developed procedures would not be expected to be particularly successful at the plate mill since it is difficult to uniformly cool the thicker plate, since distortion from flatness may result, and since plate is usually not coiled.

The influence of various cooling schedules after the hot rolling of 1/4 inch plate of structural steels modified with columbium, molybdenum, and boron has recently been reported by Cryderman, Coldren, Bell, and Grozier [46]. Strength increases resulting from the treatments were associated with grain refinement of the ferrite. Previous investigations [2] had concluded that accelerated cooling did not effectively suppress the recrystallization of austenite in carbon steel, but there was an effect when dealing with precipitation hardening steels since the presence of elements such as columbium and vanadium, which can cause precipitation, retard the completion of austenite recrystallization.

The controlled cooling of steel strip after coiling can also play an important part in the control of properties. If temperature at the coil is sufficiently high and if the austenite decomposition transformation has not been completed on the run-out table, then the transformation will continued in the coil and precipitation hardening will take place in applicably alloyed steels.

High Temperature Thermomechanical Treatment (HTMT)

Work hardening may be accomplished simultaneous with recrystallization, even if steel hot fabrication is done in the austenite single phase region. Our literature survey has shown that results include increases in values of yield strength, ultimate tensile strength, ductility, and fatigue properties, as compared with properties obtained with more conventional heat treatments. The degree of change of properties depends on the specific alloy being considered and on the variation of processing parameters. An effective HTMT has been described by Ivanova and Gordienko [47]: steel was heated well into the austenitic region (1150 - 1200°C), cooled to a temperature slightly above the A_3 line and then given 25 - 30% plastic deformation at the latter temperature. After the described thermomechanical treatment the steel was immediately water quenched and tempered in the low temperature range from 100 to 200°C. Yield strength increases were of the order of 10% to 20% as compared with the same steels given the same thermal treatments without accompanying plastic deformation. The plastic deformation was considered to be responsible for the development of a very fine microstructure. When deformed at a temperature just above the A_3 line, instead of at higher temperatures, the rate of recrystallization of austenite is comparatively slow. Quenching was done to prevent recrystallization, and to promote the martensite reaction with the applicable steels.

Koppelaar [48] in his recent survey of thermomechanical treatments as accomplished in the Soviet Union has concluded that there is a formation of carbides during HTMT when precipitation hardening steels are worked with. The solid solubility of carbon in austenite is thought

to be considerably reduced by simultaneous plastic deformation, resulting in carbide formation during HTMT. The carbides will reenter solid solution as soon as the deformation is completed unless the steel is quenched. From an industrial viewpoint HTMT is important since the deformation is accomplished at temperatures compatible with existing fabrication facilities, and no installation of new equipment would be required to accomplish the processes. Unfortunately, recrystallization cannot be completely avoided during HTMT; thus, steels with slow recrystallization kinetics, as tool steels, are considered to be [49] particularly applicable for HTMT.

Low Temperature Thermomechanical Treatment (LTMT)

The processes designated as LTMT are also referred to as "ausforming." Steels capable of forming martensite are involved, and processing consists of deforming the steel while below the recrystallization range but while at a temperature in excess of the martensite start M_s temperature. A typical LTMT is described in detail in the Russian translation [47]; the amount of plastic deformation involved was in the range from 75 to 95%.

As compared with results produced by HTMT, LTMT can give very high increases in yield strength and usually result in increased ductility, although some ductility decreases have been reported. High alloy steels are most suitable for LTMT since there is a sufficiently wide metastable austenite bay in the time-temperature cooling diagram with these steels to allow time for fabrication to be accomplished.

During processing by LTMT a number of structural changes may take place. Since the deformation temperature is below the solution

temperature for most of the carbides, deformation will be accomplished simultaneous with carbide precipitation. Another important feature of LTTMT is that during the austenite-martensite transformation the high dislocation density of the deformed austenite is retained by the martensite, resulting in strengthening.

HTTMT and LTTMT have been successfully combined in one processing schedule [48] which has been referred to as combined thermomechanical treatment or CTMT. Encouraging results have been obtained with 0.3 - 0.4 w/o C steels containing W, V, Ni, and/or Mo additions. Yield strength increases of 35 to 45% and ultimate tensile strength increases of 10 to 30% have resulted from application of CTMT, the measures of strength being compared with those resulting from conventional hot rolling [48].

Isoforming

Isoforming consists of fabrication accomplished simultaneous with the austenite-pearlite reaction. A result is the obtaining of a very fine subgrain structure in the ferrite: partial or complete spheroidization may also take place [50]. With several alloy steels only small improvements in ultimate and yield strengths were obtained by isoforming, but there were marked improvements of toughness, particularly as measured by decreases of the notch brittle-ductile transition temperature.

Preliminary Thermomechanical Treatment (PTMT)

This new processing technique appears to be one of the most interesting and potentially useful of any. Involved with PTMT is plastic deformation accomplished before austenization. It has been

established [48] that there are strengthening effects if (a) steels are cold worked before austenitization, and (b) if the cold worked steels are rapidly heated to the austenitization temperature. It appears that at least some of the dislocations introduced by prior cold work are retained during thermal processing.

CHAPTER II

MATERIAL, FABRICATION, AND SPECIMEN PREPARATION

A-441 Steel

It was decided at an early stage that the steel to be investigated in this thesis would be one of the high strength, low alloy compositions. These materials represent the new generation of structural steels, and the results of thermomechanical research and development described in the technical literature having to do with these materials is minimal. Also, the steels classified as HSLA should be capable of giving several interesting responses to thermomechanical treatments, because of the modified compositions as compared with carbon steels. As the program developed it was found that it would be possible to have three different steels fabricated by a very cooperative industrial concern (Republic Steel Corporation), and one from each of the three HSLA classes was selected:

- a. X-52, single addition (Mn)
- b. X-60, double addition (Mn,V)
- c. A-441, triple addition (Mn,V,Cu).

This thesis is concerned with A-441; X-52 is now being investigated by Mr. Y. M. Ebadi at the Georgia Institute of Technology, and X-60 will be involved in a subsequent program.

All of the A-441 steel provided by the Republic Steel Corporation for this investigation was taken from one piece of half inch thick plate

prepared and fabricated in the Republic Steel production facility in Gadsden, Alabama. The rolling schedule was proprietary and thus was not revealed to the writer, but was said to involve some commercial controlled rolling operations including hot finishing. The plate was one of the products of the heat identified as 4034124. The analyzed chemical composition included 0.12 w/o C, 0.82 w/o Mn, 0.012 w/o P, 0.027 w/o S, 0.31 w/o Cu, and 0.043 w/o V.

The Thermomechanical Treatment Program

The thermomechanical treatment programs which were developed were intended to cover as many of the previously mentioned thermomechanical treatments as were thought to be applicable to the particular steel being considered. Because of the composition limitations of A-441 (being a HSLA steel, it is not highly alloyed) it was realized that low temperature thermomechanical treatment (LTMT) was an impossibility -- the T-T-T transformation diagram of A-441 is not of a type appropriate for LTMT since metastable austenite decomposition at temperatures below the A_1 will be initiated in very short times. Since LTMT could not be done, then combined thermomechanical treatment (CTMT) was also eliminated as an experimental possibility with A-441. Controlled cooling and coiling could not be investigated since sample sizes and fabrication facilities available at the Republic Steel Research Center eliminated the possibilities of coiling. Of course, all fabrication work which was done had to be consistent with the capabilities of Republic Steel research facilities.

A comprehensive experimental fabrication program was developed which was thought to include the possibilities of accomplishing:

- a. High temperature thermomechanical treatment (HTTMT) at temperatures where all carbides should be in solution and also at temperatures at which carbide precipitation should be concurrent with fabrication. Nitrides or carbonitrides of vanadium may be involved, instead of just iron-carbides.
- b. Isoforming, temperatures being selected so that the austenite-pearlite reaction should take place simultaneous with plastic deformation by rolling.
- c. Preliminary thermomechanical treatment (PTMT), since half of the samples were cold worked before being hot or warm worked at the mill.

The fabrication program included temperature ranges which may be thought of as being unusually low, even for thermomechanical treatments, and extended well below the A_1 line; of interest were the effects of possible cold or warm work and possible aging simultaneous with deformation.

From the provided A-441 plate a total of 20 samples were prepared for inclusion in the thermomechanical treatment program. One sample was set aside and was given the code or designation, "A"; it was representative of the mill condition material, as produced in Gadsden, which was the starting material for all further processing. Sample size included the dimensions of 10 inch length by 6 inch width by thickness (half inch). The length dimension was in the rolling direction of the larger plate, and was also in the rolling direction for all further thermomechanical processing. Sample sizes were dictated by the available heating facilities adjacent to the rolling mill

at the Republic Steel Research Center and by the characteristics of the mill itself. All fabrication was accomplished in one two-high reversing mill with 14 inch diameter rolls of 20 inch effective length, and the mill was operated to give a roll velocity of 1,000 rpm.

Ten of the samples were given a preliminary 20% reduction, to 0.40 inch thickness, by cold rolling at room temperature; these included the materials to be involved in the preliminary thermomechanical treatment (PTMT) program as modified by other subsequent operations. One of the samples was designated as "B" and was set aside to be representative of the cold worked A-441. The other nine samples were each introduced into a furnace at high temperature (2000, 1850, 1700, 1551, 1400, 1250, 1100, 950, and 800°F), were held in the furnace for one hour, and were then removed from the furnace and as rapidly as possible reduced another 20% in thickness, to 0.32 inch, in one pass through the rolling mill. This group of samples, a total of 10 including B, will hereafter be referred to as the "cold work-hot work" material.

The nine remaining samples, each in the mill condition, and thus with a thickness of one-half inch, were introduced into a furnace at high temperature (the same temperatures as mentioned in the last paragraph), were held at furnace temperature for one hour, and were then as rapidly as possible reduced to a final gage of 0.32 inch; two passes, each giving 20% reduction, were made. Only a few seconds elapsed between passes, so that there was but little opportunity for temperature changes. This group of samples will hereafter be referred to as the "hot-work" material.

Codes involving identification letters for the various samples are summarized in Table 1: samples A and B, respectively, were

representative of the mill condition and 20% cold worked A-441.

Table 1. Code or Designation of Fabrication Samples

Furnace Temperature, °F	Group 1 "Cold Work-Hot Work"	Group 2 "Hot Work"
800	C	L
950	D	M
1100	E	N
1250	F	O
1400	G	P
1550	H	R
1700	I	S
1850	J	T
2000	K	V

Care was taken to insure that all samples were cooled from fabrication temperatures under rather identical conditions. Just as rolling was completed, while the sample was still at temperature, each plate was placed in a granular material specifically provided for cooling purposes.

Preparation of Test Specimens

Charpy Specimens

All test specimens were prepared in the Materials Processing Laboratory of the School of Mechanical Engineering, Georgia Institute of Technology, by the writer of this thesis. Assistance and guidance was given by acknowledged machine shop personnel. Machining operations were carefully and conservatively done, so as to avoid distortion or heating which would alter mechanical properties.

As an initial operation about one inch of material was removed from each plate by a single saw cut made with a power hack-saw. This

end material was discarded since it was thought that it might not be representative of the bulk of the plate due to end effects resulting from fabrication and heating. In the next operation a 2-1/4 inch long piece was cut in a single operation of the power hack-saw. This piece, as indicated by Figure 1, was to be used for the preparation of Charpy specimens. The plate section was surface ground to Charpy specimen length (55 mm) while using a Blohm-Simplex 5 surface grinder with a 12 inch diameter wheel. Grind depth in all operations with this unit was limited to a maximum of 0.005 inch, in order to avoid overheating, and an adequate supply of water cooling was maintained during grinding to insure that room temperature machining was being accomplished. With the same grinding unit the plate section was also reduced to 0.263 inch thickness, a value which is two-thirds of the thickness of a "standard" Charpy specimen. Full thickness (10 mm) specimens could not be prepared because of the fabricated thickness of the plate (0.32 inch), and two-thirds thickness is a standard compatible with steel industry practice for sheet and thin plate. Blanks for the final preparation of Charpy specimens were saw cut from the ground plate sample by use of a DoAll Metalmaster band saw with a blade of 1/4 inch depth and 14 teeth per inch. Each Charpy blank was given a number, indicated in Figure 1, to allow the identification of location in the plate and was also stamped at the ends with the appropriate letter designation of Table 1. After the grinding of saw cut surfaces to give the desired Charpy width of 10 mm, a standard V-notch of two mm depth was machined by the use of a specially prepared cutter mounted on a Milwaukee Model H horizontal milling machine. Final dimensions of the Charpy specimens conformed

to ASTM Standard E-23, and dimensions are indicated on Figure 2.

Tensile Specimens

Two longitudinal rolling direction blanks and one transverse blank were saw cut from the remaining plate, at the locations indicated by Figure 1, for the eventual preparation of tensile specimens. All blanks were approximately 5/8 inch in width. As the next operation the blanks were rough turned to half inch diameter on a Monarch Model 12 CK lathe; of course the piece which resulted was not completely round, since the plate thickness was only 0.32 inch. Ends were threaded over a length of about one inch (1/2 inch diameter, 13 threads per inch), and due to the plate thickness there were flats on opposite sides of the threaded ends. The gage section of each test specimen was machined in a Monarch Model 14 C lathe equipped with a True-Trace Model 106 633 tracer attachment. The final dimensions of the tensile test specimens are also indicated by Figure 2, and these dimensions are in accord with ASTM Standard E-8. Previous experience, verified by preliminary experimentation, had shown that the 0.252 inch diameter specimens would deform and fail in the gage length and not in the threaded ends with reduced cross-sectional areas resulting from the large flats consistent with 0.32 inch plate thickness.

Metallographic Specimens

Metallographic specimens were prepared by rather standard procedures applicable for plain carbon steels of equivalent carbon content. The metallographic specimens extended across the thickness of the plate, from surface to surface, were of about one-half inch length in the rolling direction, and had their planes of polish parallel with the rolling

direction. Specimen locations are indicated by Figure 1. Grinding, polishing, and etching were done in the Metallography Laboratory of the School of Mechanical Engineering. Bakelite mounted specimens were ground with AB Carbimet Silicon Carbide papers with grits including 180, 240, 320, 400, and 600. Polishing was done on 8 inch diameter wheels with Buehler AB Microcloth; rough polishing was done with Buehler Alpha Micropolish, 0.3 micron, and final polishing with Buehler Gamma Micropolish, 0.05 micron. A standard 3% Nital solution was used for etching. All were repolished and etched several times, to give optimum phase contrast.

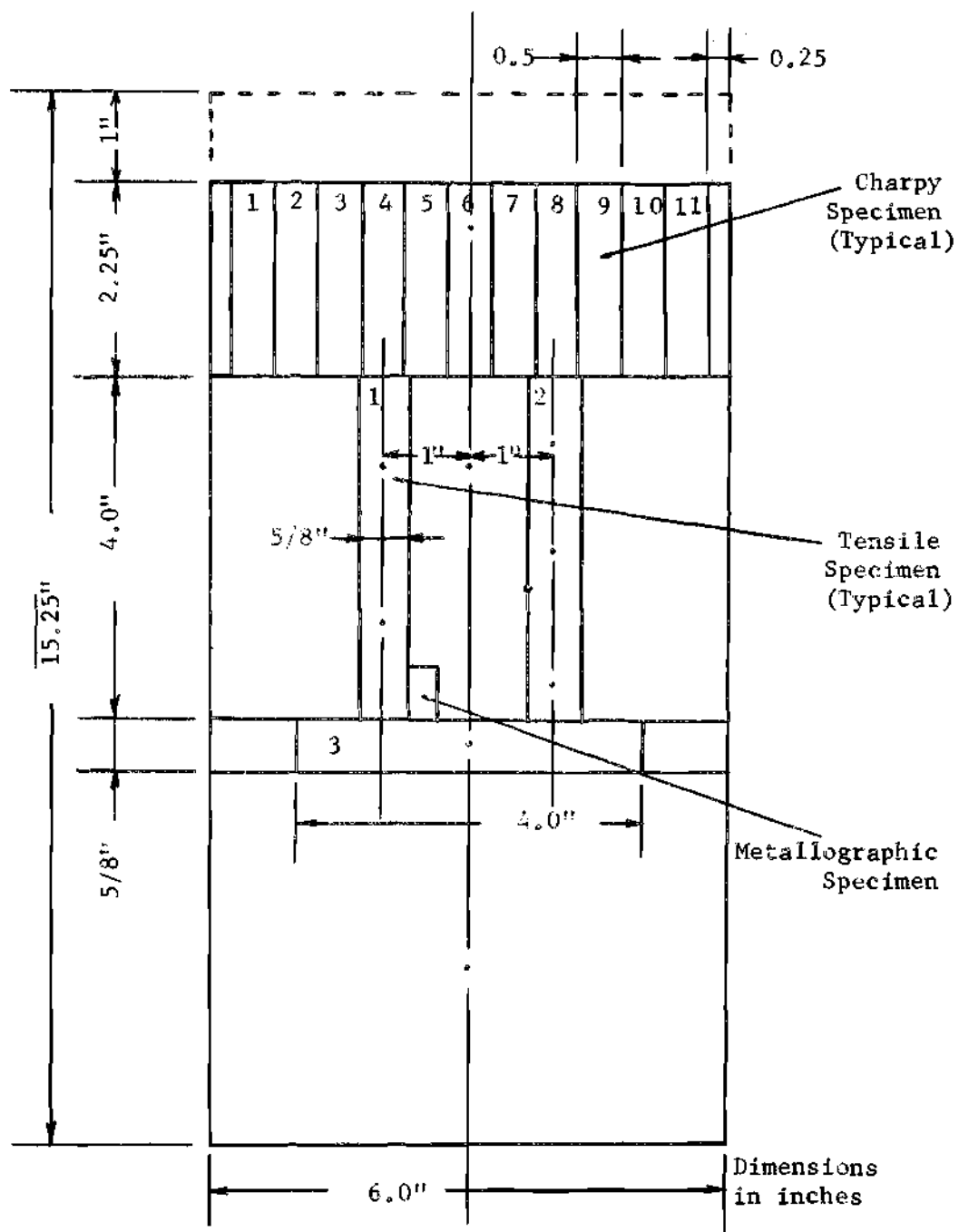
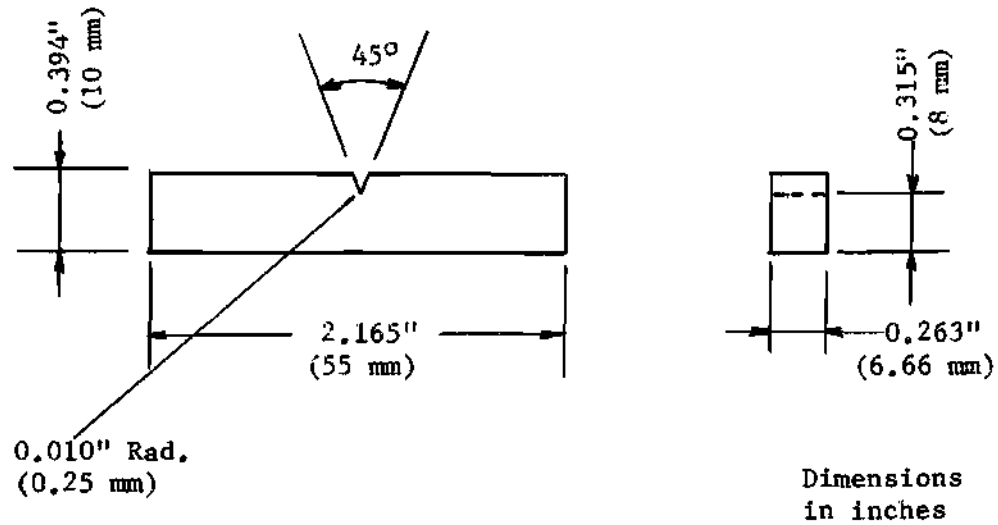


Figure 1. Location of Test Samples Relative to Fabricated Plate

Charpy V-Notch Specimen



Tensile Specimen

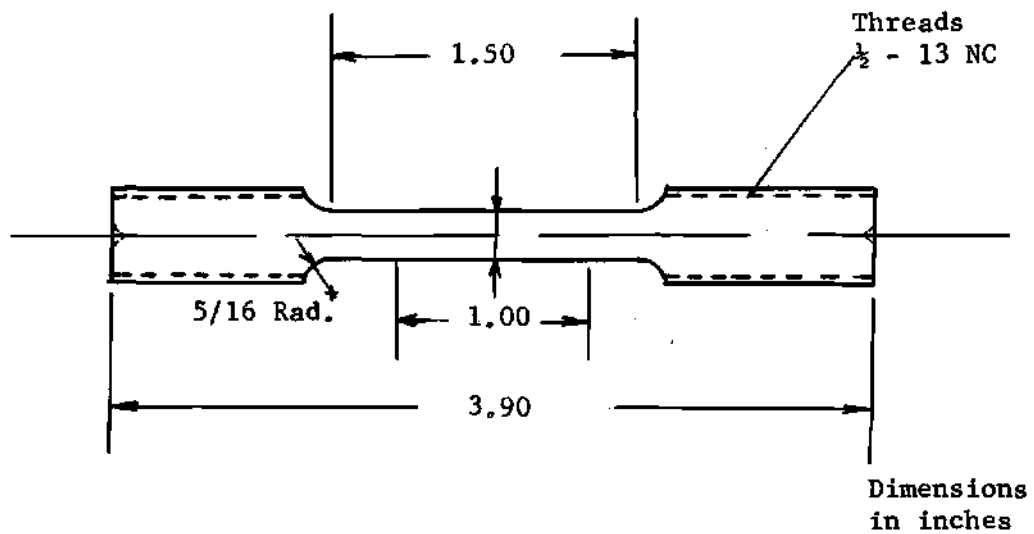


Figure 2. Test Specimen Dimensions

CHAPTER III

EXPERIMENTAL PROCEDURES

Tensile Tests

Thesis tensile testing was done in the 10,000 pound capacity floor model Instron machine of the School of Mechanical Engineering. The machine is physically located in Room 108 of Space Sciences and Technology 1 Building. Only ambient temperatures were considered, and a crosshead velocity of 0.05 inch per minute was held constant during all thesis work.

The School of Mechanical Engineering Model TTC Instron machine is a unit complete with sophisticated instrumentation. Load-elongation diagrams are autographically recorded on 10 inch wide chart paper when an appropriate extensometer is properly attached to test specimens. Motion of the pen across the ten inch width of the chart paper is actuated by the signal from a load cell, while x-direction pen travel is proportional to the elongation signal from the extensometer. In the testing of thesis material the Instron machine was operated at either 10,000 pound or 5,000 pound capacity, depending on the code designation of the steel being elongated, while the extensometer range was correspondingly set for either 25% or 50% maximum elongation. The Instron Model G51-12 extensometer was exclusively used, since it was capable of achieving elongation values consistent with the steel samples being tested. The mentioned combinations of load capacity settings and extensometer settings result in load-elongation diagrams of maximum size.

Pertinent dimensions of the tensile test specimens were precisely measured before and after testing, with micrometers being the most commonly used measuring instruments, although on several occasions an optical comparator was also utilized. Results obtained by direct calculation from results plotted on the load-elongation diagrams included upper yield point and lower yield point values, when applicable, or 0.2% offset yield strength. Yield point elongation was directly measured from those diagrams which showed discontinuous yielding. Uniform elongation, to the onset of necking, was also measured from the charts, as was total elongation to fracture. Specimen diameter at the fracture was determined, by micrometer or optical comparator, and percent reduction of area values were then calculated. Values of engineering fracture stress were obtained by noting the fracture load and dividing by initial specimen cross-sectional area; true fracture stress values were based on the measured specimen diameter at fracture.

Each recorded load-elongation diagram was considerably analyzed as regards strain hardening. In most cases the value of load on each diagram was noted at each percent of plastic strain; for those test specimens which were found to be in hardened conditions, and which thus showed but little ductility before fracture, load values were determined at each half percent value of strain. Each value of load was converted to engineering stress, by dividing by the initial cross-sectional area, and engineering stress-strain data for each specimen was then compiled in tabular form. True stress and true strain values, corresponding to the individual engineering stress and strain values, were then calculated by application of appropriate and elementary formulations; of

course, such conversions can only be made for those loads and elongations measured before the onset of necking.

Difficulties were encountered when calculating values of the strain hardening coefficient n and the strength coefficient K , both being defined by Equation 14. The difficulties resulted from the fact that when $\log \bar{\sigma}$ values were plotted against $\log \bar{\epsilon}$ values, for one given test, exact linearity usually was not found, as is demanded by Equation 14. It was finally decided that two sets of n and K values would be obtained for each tested specimen. One set of n and K values was calculated by evaluating the slope of the $\log \bar{\sigma}$ - $\log \bar{\epsilon}$ diagrams at the maximum loads as indicated by the strip chart records, to give n values, and by then using these n values and the maximum load values with Equation 14 to calculate K values. The other set of n and K values were obtained by using Considere's finding that the true uniform elongation has a value equal to n (when Equation 14 is exactly followed), and then by using these values of n with maximum load values to calculate K values from Equation 14. The two sets of n and K values so calculated for each test specimen generally showed little deviation, but appreciable differences were noted for the cases involving severely cold worked materials.

The tensile testing and subsequent evaluation program involved with this thesis was large. There were an initial total of 60 test specimens, and the results from each had to be analyzed by indicated means. As is nearly always the case with a program of this scope, some of the tensile specimens necked and fractured at the fillets at the ends of gage lengths, instead of in the gage lengths; all

deformation after necking is then accomplished outside of the gage length of the extensometer. Necking at fillets is no doubt a direct result of undercutting by the tracer lathe. For those cases where necking and fracture did take place at the ends of gage lengths, at the fillets, duplicate tests were run with specimens machined after the initial machine shop program.

Charpy Impact Tests

A total of 220 V-notch Charpy specimens, 11 from each of 20 code designations, were available for testing. Since there is a considerable hazard associated with operation of Charpy machines, all testing was done by a group of three investigators including Professor Clough and Mr. Ebadi. The 220 foot-pound capacity Tinius Olsen Charpy-Izod unit belonging to the School of Mechanical Engineering, but housed in an Engineering Science and Mechanics laboratory, was exclusively used.

The primary objective of impact testing was the determination of Charpy energy values over the entire transition temperature range, from very brittle behavior to very ductile behavior, so as to allow evaluation of the 15 foot-pound transition temperature for each code designation. It was found that A-441 steel is of a type not amenable to determinations of fracture appearance transition temperatures, so the Charpy evaluations involved only energy values.

Required variations of test temperature were obtained by liquid baths confined in well insulated wide-mouth Thermos flasks. Specimens were immersed in the appropriate liquid baths for at least 30 minutes before being tested. Elapsed time between specimen removal from the bath and rupturing of the test bars by the Charpy machine was less than

two seconds, giving but little opportunity for change of temperature from the rather stable bath temperature.

Water was utilized as the bath for elevated temperature testing. Temperatures below room temperature were obtained by using controlled mixtures or solutions of ice and water, ice and water and table salt, dry ice and acetone, or liquid nitrogen and ethyl alcohol. Once the proper concentrations or mixtures were obtained remarkably stable temperatures resulted; one bath of dry ice and acetone, with sufficient dry ice to give -30°F , retained this temperature within one degree Fahrenheit when left overnight. Thermometers calibrated in undergraduate laboratories were used to measure temperatures of the baths; each of the thermometers could be read to within one-half degree.

Energy values obtained with the eleven Charpy specimens of each material code given in Table 1 were plotted against testing temperature, and the 15 foot-pound transition temperature was directly read from the plots.

Hardness Tests

All hardness evaluations were accomplished with units installed in the specimen preparation room of the Metallography Laboratory, School of Mechanical Engineering. Available there is a Brinell unit manufactured by the Steel City Testing Laboratory of the Tinius Olsen Testing Machine Company. All Brinell determinations of hardness involved the application of 3,000 kg loads to 10 mm diameter spherical indentors; the mentioned combination of diameter and load is the most common for steel specimens.

Also available in the same laboratory is a Rockwell unit made

by the Wilson Mechanical Instrument Division, American Chain and Cable Company. As previously mentioned, Rockwell indentations were made on the larger sides of ruptured Charpy specimens since the machined surfaces available there are ideal for such testing. Care was taken to avoid the strain hardened material adjacent to fracture surfaces. At least 10 Rockwell hardness determinations were made for each code designation listed in Table 1. The B scale was found to be applicable for the majority of the various code designations, and operation was then with the usual 1/16 inch diameter ball and 100 kg major load. Some code designations were harder than the upper limit of the B scale, which is 100 R_b, and for these the C scale, with diamond brale and 150 kg major load, was utilized.

Metallographic Analyses

In the Metallographic Laboratory of the School of Chemical Engineering a minimum of four photomicrographs were prepared from each of the polished and etched metallographic samples. The primary unit for the high magnification optical investigations was a vertical Vickers "55" metallograph. The majority of photomicrographs were prepared at either 100, 200, or 400x magnification, but observations were also made at other magnifications. Sheet film, four inch by five inch, was used, and the long dimension of the film was oriented to be in the rolling direction of the plate. Panatomic X and Tri-X Ortho films were used and both were developed in DK-50. Contact prints were made in the School of Mechanical Engineering darkroom, with both Velox F4 and Azo F5 contact papers being used, the latter for increased contrast.

Unless a particular, local, peculiarity or characteristic was being observed, every effort was made to have each photomicrograph be representative of the entire structure. Initial observations showed that little if any decarburization had occurred at plate surfaces; in fact, there was generally but little variation in microstructure through thicknesses of plate samples fabricated in the experimental rolling program.

Photomicrographs were made to allow quantitative measures to be associated with those features which might be expected to influence mechanical behavior. For example, the Hall-Petch relationship, Equation 1, indicates that ferrite grain size would be expected to be an important parameter to be evaluated by quantitative metallography.

Similarly, Equation 7 indicates that both grain size and volume fraction of pearlite would influence yield strength values, if an applicable steel in an appropriate condition were considered, while Equations 8-10 indicate that the ultimate tensile strength might be influenced by the same two quantities. Other previously discussed relationships (Equations 11-13) taken from the literature indicate other possible variations of properties with microstructural changes. Cold or warm work would no doubt result in a departure from an equiaxed grain structure, resulting in grain elongation in the rolling direction, and a quantitative measure of this degree of orientation could be of importance.

The volume fraction of pearlite was established by the well known point counting method. A transparent grid consisting of sharp dark lines intersecting to make 1/4 inch squares was used for all

quantitative metallographic analyses; the grid size was recommended by Dr. E. E. Underwood who showed a special interest in this thesis. The grid was placed over photomicrographs so as to have one set of lines in the rolling direction, the other set then being in the transverse direction. In the grid on the photomicrograph the grid lines will intersect in a certain number of points, the number for a particular grid being dependent on the size of the photomicrograph. The volume fraction of pearlite will simply be the number of grid intersection points over pearlite features divided by the total number of points, while the volume fraction of ferrite is the number of grid intersection points over ferrite grains divided by the total number of points. If only ferrite or pearlite were present in the microstructure, the sum of the volume fractions would be one. Actually, some of the grid intersection points might be over inclusions, as manganese-sulfide, or might be associated with spheroidized cementite.

The previously described grid was also employed to establish values of the grain diameter d and to evaluate other quantities as well. Incidentally, the grain diameter d is perhaps better referred to as the "mean intercept length"; it will be the average length of random line intercepted by the average grain. Using Underwood's [51] symbols and notations, the ferrite mean intercept length would be given by:

$$d_{\alpha} = \frac{\% \text{ Ferrite}}{100} \times \frac{1}{N_{L\alpha}} \quad [\text{in}] \quad (16)$$

In this relationship $N_{L\alpha}$ is the number of interceptions of ferrite grains per unit of length of grid line (inch^{-1}). For our specific case, since we would expect to have a ferrite-pearlite microstructure,

the quantity N_L is defined as [51]:

$$N_{L\alpha} = \frac{2(P_L)_{\alpha\alpha} + (P_L)_{\alpha\beta}}{2} \quad [\text{in}^{-1}] \quad (17)$$

where $(P_L)_{\alpha\alpha}$ = number of ferrite-ferrite interfaces (grain boundaries)
per unit length of grid line

$(P_L)_{\alpha\beta}$ = number of ferrite-pearlite interfaces per unit length
of grid line

Similar relationships may be used to evaluate the pearlite mean intercept, which would be:

$$d_\beta = \frac{(\% \text{ Pearlite})}{100} \times \frac{1}{N_{L\beta}} \quad [\text{in}] \quad (18)$$

where $N_{L\beta}$ = number of interceptions of pearlite colonies
or patches per unit length of grid line

Since at the moment we are not interested in the number of ferrite grains, Equation 17 becomes:

$$N_{L\beta} = \frac{(P_L)_{\alpha\beta}}{2} \quad [\text{in}^{-1}] \quad (19)$$

The orientation factor Ω is an indication of the degree of distortion of the ferrite grains, and Underwood's defining relationship is:

$$\Omega_\alpha = \frac{(N_{L\alpha})_\perp - (N_{L\alpha})_\parallel}{(N_{L\alpha})_\perp + 0.571 (N_{L\alpha})_\parallel} \quad (20)$$

where $(N_{L\alpha})_\perp$ = number of interceptions of ferrite grains of the
microstructure per unit of length of grid lines
normal to the rolling direction,

$(N_{L\alpha})_\parallel$ = number of interceptions of ferrite grains of the

microstructure per unit length of grid lines
parallel to the rolling direction.

Note that for a perfectly oriented structure, corresponding to a hypothetical microstructure in which the grains are reduced to lines in the rolling direction, that Ω_α will have a value of one. When grains are ideally equiaxed the value of the ferrite orientation factor will be zero. For a partially oriented structure the orientation factor will have values between these limits.

As mentioned before, the same grid that was used for pearlite determinations, while similarly oriented with respect to photomicrographs, was used to calculate the basic variables of Equations 17, 19 and 20; however, the technique was considerably different. In this case, it was necessary to count the number of microstructural features, as ferrite-ferrite interfaces and ferrite-pearlite interfaces, cutting grid lines, so that the number of features per unit length of grid line may be calculated. This counting procedure was made separately in the rolling direction and transverse to the rolling direction as required by the basic variables in Equation 20. The following formulation and definition were used for P_L determination:

$$(P_L)_{\alpha\alpha} = \frac{(P_{\alpha\alpha})_{||} + (P_{\alpha\alpha})_{\perp}}{L_{||} + L_{\perp}} \quad (21)$$

where

$L_{||}$ = length of the rolling direction grid lines

L_{\perp} = length of the transverse grid lines

$(P_{\alpha\alpha})_{||}$ = total number of intersections of ferrite-ferrite grain boundaries with rolling direction grid lines

$(P_{\alpha\alpha})_{\perp}$ = total number of intersections of ferrite-ferrite grain boundaries with transverse grid lines.

similar to Equation 21 there can be written:

$$(P_L)_{\alpha\beta} = \frac{(P_{\alpha\beta})_{||} + (P_{\alpha\beta})_{\perp}}{L_{||} + L_{\perp}} \quad (22)$$

The various symbols indicate the same quantities as in Equation 21, except that with Equation 22, it is the ferrite-pearlite interfaces which are considered.

CHAPTER IV

RESULTS

Mechanical PropertiesTensile Tests

Calculated results obtained by consideration of all of the Instron plotted load-elongation diagrams are summarized in Tables 2, 3, 4, 5, 6, and 7. Even-numbered tables contain results for the "hot-work" code designations, while odd-numbered tables treat the results obtained with "cold work-hot work" samples. Tables 2 and 3 consider those properties involved with yielding while Tables 4 and 5 primarily consider the calculated properties associated with necking. Tables 6 and 7 have to do with properties at the fracture stage.

Charpy Impact Tests

Energy values (foot-pounds) obtained with all of the V-notch Charpy specimens are listed in Tables 8 and 9; the former treats those samples prepared from "hot work" material, while the latter has to do with "cold work-hot work" A-441. For the steel of each code designation, Charpy energy was plotted as the ordinate against testing temperature as the abscissa, and values of 15 foot-pound transition temperatures were obtained from these plots. The values of 15 foot-pound transition temperatures so determined are given in Table 10.

Hardness Tests

Rockwell B (R_B) and Rockwell C (R_C) test results have been included in Tables 11 and 12. Each listed result is the average of ten

determinations made for each of the code designated steels. The results of Brinell tests made with 3,000 kg loads and 10 mm diameter balls are also included in Table 12, and each listed value represents the results of three determinations.

Metallographic Analyses

Quantitative metallographic results obtained from the photomicrographs are listed in Tables 13 and 14, the results being listed for each individual photomicrograph which was analyzed. Included are values of the ferrite mean intercept (grain diameter), volume fraction of pearlite as expressed on a percent basis, and ferrite orientation factor. Also included in Tables 13 and 14 are calculated values of $d^{-\frac{1}{2}}$ which is one of the terms to appear in the Hall-Petch relationship and its modifications.

Table 2. Tensile Test Results Related
to Yielding, Hot Work Samples

Code	Finishing Temperature (°F)	Upper Yield Point (psi)	Lower Yield Point (psi)	0.2% Offset Yield Strength (psi)	Yield Point Drop (psi)	Yield Point Elongation %
Longitudinal Specimens						
A1	mill	56,290	51,480	---	4,810	1.3
A2	mill	56,090	50,480	---	5,610	1.3
L1	800	---	---	119,940	---	---
L2	800	---	---	120,780	---	---
M1	950	---	---	95,980	---	---
M2	950	---	---	96,930	---	---
N1	1100	84,320	84,020	---	300	0.5
N2	1100	---	---	84,840	---	---
O1	1250	74,610	73,510	---	1,110	1.3
O2	1250	76,740	75,640	---	1,100	1.3
P1	1400	66,370	60,740	---	5,630	2.4
P2	1400	65,620	60,120	---	5,500	2.4
R1	1550	63,350	54,920	---	8,430	2.5
R2	1550	66,860	56,570	---	10,290	2.8
S1	1700	61,720	56,800	---	4,920	1.8
S2	1700	59,190	56,590	---	2,600	1.8
T1	1850	61,370	56,460	---	4,910	1.5
T2	1850	63,160	56,960	---	6,200	1.3
V1	2000	55,330	53,920	---	1,410	1.0
V2	2000	55,170	53,770	---	1,400	1.0
Transverse Specimens						
A3	mill	58,870	52,320	---	6,550	1.2
L3	800	---	---	119,810	---	---
M3	950	95,840	95,840	---	---	0.4
N3	1100	91,590	91,590	---	---	0.4
O3	1250	77,360	74,760	---	2,600	1.0
P3	1400	66,100	62,270	---	3,830	2.4
R3	1550	63,580	59,880	---	3,700	2.6
S3	1700	60,260	55,760	---	4,500	1.9
T3	1850	63,530	59,140	---	4,390	1.2
V3	2000	56,920	54,110	---	2,810	1.0

Table 3. Tensile Test Results Related to
Yielding, Cold Work-Hot Work Samples

Code	Finishing Temperature (°F)	Upper Yield Point (psi)	Lower Yield Point (psi)	0.2% Offset Yield Strength (psi)	Yield Point Drop (psi)	Yield Point Elongation %
Longitudinal Specimens						
B1	Cold Rolled	---	---	93,150	---	---
B2	Cold Rolled	---	---	89,950	---	---
C1	800	---	---	112,660	---	---
C2	800	---	---	113,180	---	---
D1	950	---	---	101,570	---	---
D2	950	---	---	102,540	---	---
E1	1100	---	---	85,040	---	---
E2	1100	---	---	85,250	---	---
F1	1250	66,500	65,190	---	1,310	1.4
F2	1250	66,460	64,260	---	2,200	1.35
G1	1400	64,530	60,860	---	3,670	1.9
G2	1400	62,880	57,350	---	5,530	2.0
H1	1550	71,550	62,760	---	8,790	2.9
H2	1550	70,200	62,210	---	7,990	2.9
I1	1700	60,610	56,710	---	3,900	1.4
I2	1700	60,490	55,850	---	4,640	1.6
J1	1850	56,330	54,430	---	1,900	1.0
J2	1850	56,310	54,500	---	1,810	1.0
K1	2000	53,960	53,360	---	600	0.9
K2	2000	53,020	53,020	---	---	0.9
Transverse Specimens						
B3	Cold Rolled	---	---	87,250	---	---
C3	800	---	---	110,980	---	---
D3	950	---	---	100,770	---	---
E3	1100	---	---	90,730	---	---
F3	1250	---	---	68,450	---	---
G3	1400	63,980	60,480	---	3,500	2.1
H3	1550	61,500	59,890	---	1,610	2.0
I3	1700	61,890	56,430	---	5,460	1.5
J3	1850	59,700	55,640	---	4,060	1.1
K3	2000	55,330	53,930	---	1,400	0.7

Table 4. Tensile Test Results Related
to Necking, Hot Work Samples

Code	Finishing	Ultimate	Uniform	Strain Hardening		Strength	
	Temperature	Tensile	Elongation	Exponent		Coefficient K	
	(°F)	Strength	%	UTS	Graph.	UTS	Graph.
Longitudinal Specimens							
A1	Mill	75,320	17.0	0.1570	0.1573	117,850	117,920
A2	Mill	74,920	17.0	0.1570	0.1564	117,230	117,070
L1	800	124,530	2.5	0.0247	0.0221	139,850	138,520
L2	800	124,400	2.2	0.0218	0.0202	138,170	137,350
M1	950	106,580	5.8	0.0559	0.0536	132,430	131,550
M2	950	106,520	5.8	0.0559	0.0510	132,360	130,480
N1	1100	96,120	7.5	0.0723	0.0688	124,950	123,790
N2	1100	97,510	7.0	0.0676	0.0760	125,180	127,980
O1	1250	86,340	9.3	0.0889	0.0905	117,030	117,480
O2	1250	88,400	9.6	0.0917	0.0922	120,620	120,770
P1	1400	78,240	16.5	0.1527	0.1480	121,450	120,360
P2	1400	78,180	16.5	0.1527	0.1542	121,350	121,680
R1	1550	76,000	18.8	0.1723	0.1573	122,240	118,990
R2	1550	75,950	18.5	0.1697	0.1620	121,630	119,940
S1	1700	78,280	17.4	0.1604	0.1538	123,250	121,770
S2	1700	78,080	17.0	0.1570	0.1385	122,180	117,930
T1	1850	78,720	16.0	0.1484	0.1517	121,210	121,950
T2	1850	79,080	15.0	0.1398	0.1384	119,730	119,390
V1	2000	78,960	15.0	0.1398	0.1408	119,540	119,800
V2	2000	79,150	15.5	0.1441	0.1481	120,860	121,800
Transverse Specimens							
A3	Mill	76,110	15.7	0.1458	0.1469	116,600	116,830
L3	800	129,110	2.9	0.0286	0.0300	147,070	147,830
M3	950	107,950	4.7	0.0459	0.0484	130,200	131,180
N3	1100	103,420	5.5	0.0535	0.0785	127,610	136,610
O3	1250	85,680	7.5	0.0723	0.0868	111,370	115,540
P3	1400	79,200	15.5	0.1441	0.1386	120,940	119,630
R3	1550	78,780	18.2	0.1672	0.1660	125,510	125,310
S3	1700	76,550	16.7	0.1544	0.1473	119,200	117,590
T3	1850	82,310	15.2	0.1415	0.1445	125,040	125,790
V3	2000	78,040	15.2	0.1415	0.1406	118,560	118,370

Table 5. Tensile Test Results Related to
Necking, Cold Work-Hot Work Samples

Code	Finishing	Ultimate	Uniform	Strain Hardening		Strength	
	Temperature	Tensile	Elongation	Exponent		Coefficient K	
	(°F)	Strength	%	UTS	Graph.	UTS	Graph.
<hr/>							
<hr/>							
Longitudinal Specimens							
B1	Cold Rolled	96,370	1.0	0.0099	0.0151	100,890	104,221
B2	Cold Rolled	96,070	1.0	0.0099	0.0140	100,580	103,442
C1	800	118,780	3.8	0.0373	0.0415	139,391	141,287
C2	800	118,450	3.8	0.0373	0.0402	138,995	140,348
D1	950	110,830	5.5	0.0535	0.0513	136,760	135,880
D2	950	110,780	5.5	0.0535	0.0548	136,700	137,210
E1	1100	97,580	7.5	0.0723	0.0849	126,840	130,980
E2	1100	97,010	7.6	0.0732	0.0737	126,410	126,561
F1	1250	79,760	11.0	0.1044	0.1028	112,080	111,680
F2	1250	78,070	11.0	0.1044	0.1034	109,710	109,460
G1	1400	81,010	15.0	0.1398	0.1299	122,660	120,240
G2	1400	76,860	15.0	0.1398	0.1296	116,370	114,030
H1	1550	79,340	17.5	0.1613	0.1643	125,130	125,810
H2	1550	78,680	16.0	0.1484	0.1530	121,140	122,200
I1	1700	79,410	15.5	0.1441	0.1464	121,250	121,800
I2	1700	78,430	16.0	0.1484	0.1512	120,760	121,390
J1	1850	79,140	15.3	0.1424	0.1418	120,440	120,290
J2	1850	79,290	15.0	0.1398	0.1308	120,040	117,920
K1	2000	79,830	14.0	0.1310	0.1399	118,780	120,910
K2	2000	79,680	14.0	0.1310	0.1380	118,560	120,220
<hr/>							
Transverse Specimens							
B3	Cold Rolled	98,210	1.7	0.0169	0.0228	107,000	109,535
C3	800	122,270	3.2	0.0315	0.0357	140,700	142,750
D3	950	112,210	4.7	0.0459	0.0401	135,340	132,880
E3	1100	101,770	6.5	0.0630	0.0830	129,010	126,210
F3	1250	81,510	8.5	0.0816	0.0824	108,500	108,720
G3	1400	81,110	14.5	0.1354	0.1322	121,750	120,950
H3	1550	79,710	14.6	0.1363	0.1441	119,860	121,720
I3	1700	78,580	15.0	0.1398	0.1349	118,960	117,840
J3	1850	79,800	15.0	0.1398	0.1412	120,830	121,180
K3	2000	79,880	14.0	0.1310	0.1304	118,860	118,680

Table 6. Tensile Test Results Related to
Fracture, Hot Work Samples

Code	Finishing Temperature (°F)	Engineering Fracture Stress (psi)	True Fracture Stress (psi)	Reduction of Area %	Elongation %
Longitudinal Specimens					
A1	Mill	51,480	145,530	64.6	31.8
A2	Mill	51,080	152,240	66.4	32.5
L1	800	87,010	172,604	49.6	10.9
L2	800	87,820	177,070	49.6	10.7
M1	950	75,280	147,360	48.9	16.2
M2	950	76,940	173,580	55.7	15.7
N1	1100	68,210	168,310	59.5	18.8
N2	1100	69,960	165,630	57.8	18.2
O1	1250	57,560	158,130	63.6	24.8
O2	1250	60,400	175,350	65.6	22.7
P1	1400	52,090	170,510	69.5	31.9
P2	1400	52,850	172,040	69.3	30.4
R1	1550	52,610	168,380	68.7	33.2
R2	1550	52,270	167,950	68.9	34.3
S1	1700	53,590	168,670	68.2	34.6
S2	1700	53,090	172,630	69.2	32.4
T1	1850	53,750	168,550	68.1	31.1
T2	1850	54,950	166,560	67.0	29.8
V1	2000	53,720	174,200	69.2	29.8
V2	2000	54,170	175,060	69.1	30.2
Transverse Specimens					
A3	Mill	60,580	147,010	58.8	27.4
L3	800	108,210	155,280	30.3	6.4
M3	950	88,780	139,990	36.6	10.5
N3	1100	86,580	141,410	38.8	11.8
O3	1250	70,750	133,260	46.9	16.7
P3	1400	63,690	156,670	59.3	27.7
R3	1550	65,980	151,790	56.5	30.2
S3	1700	63,960	144,470	55.7	27.6
T3	1850	67,930	153,010	55.6	26.4
V3	2000	58,630	153,420	61.8	28.4

Table 7. Tensile Test Results Related to
Fracture, Cold Work-Hot Work Samples

Code	Finishing Temperature (°F)	Engineering Fracture Stress (psi)	True Fraction Stress (psi)	Reduction of Area %	Elongation %
Longitudinal Specimens					
B1	Cold Rolled	65,730	164,730	60.1	14.0
B2	Cold Rolled	65,470	163,690	60.0	14.2
C1	800	82,540	184,550	55.3	13.5
C2	800	82,350	178,460	53.9	13.2
D1	950	78,640	177,080	55.6	15.8
D2	950	79,420	176,970	55.1	15.8
E1	1100	67,090	176,610	62.0	19.4
E2	1100	65,850	176,260	62.6	20.4
F1	1250	50,220	171,230	70.7	26.5
F2	1250	50,050	166,780	70.0	25.6
G1	1400	52,920	183,230	71.1	30.0
G2	1400	51,110	169,330	69.8	30.1
H1	1550	52,360	179,210	70.8	33.3
H2	1550	53,120	174,430	69.5	31.0
I1	1700	55,510	170,140	67.4	29.0
I2	1700	53,630	165,220	67.5	30.9
J1	1850	54,430	161,040	66.2	31.0
J2	1850	54,600	163,560	66.6	29.6
K1	2000	54,160	166,980	67.6	29.0
K2	2000	55,620	170,440	67.4	26.8
Transverse Specimens					
B3	Cold Rolled	75,580	141,260	46.5	10.6
C3	800	101,340	148,720	31.9	7.4
D3	950	95,150	150,950	37.0	10.0
E3	1100	84,310	142,710	40.9	13.3
F3	1250	64,800	128,000	49.4	18.2
G3	1400	65,690	149,360	56.0	25.8
H3	1550	64,010	148,670	56.9	27.0
I3	1700	64,620	148,740	56.5	26.1
J3	1850	64,170	148,710	56.8	26.1
K3	2000	64,790	144,010	55.0	25.4

Table 8. Charpy Test Results,
Hot Work Samples

Code	Temperature (°F)	Energy (Ft-lb.)	Code	Temperature (°F)	Energy (Ft-lb.)
A7	-105	5.0	L6	-105	2.0
A10	- 75	4.0	L11	- 25	2.0
A1	- 70	22.0	L7	+ 3	4.0
A2	- 50	29.5	L9	+ 16	3.0
A11	- 60	6.0	L3	+ 32	4.5
A9	- 25	44.0	L2	+ 55	7.0
A8	+ 2	52.0	L1	+ 65	22.0
A3	+ 32	46.0	L4	+ 75	18.0
A6	+ 75	69.0	L10	+ 87	12.0
A5	+212	62.0	L8	+100	26.0
			L5	+212	21.0
M6	-105	2.0	N6	-105	2.5
M9	- 50	2.0	N10	- 75	3.5
M8	- 25	4.0	N9	- 50	4.0
M10	- 12	5.0	N11	- 37	3.5
M11	0	9.0	N1	- 25	6.0
M7	+ 3	19.0	N8	- 25	30.0
M1	+ 17	13.0	N2	- 12	16.0
M3	+ 32	16.0	N7	+ 3	24.0
M2	+ 55	26.0	N3	+ 32	30.0
M4	+ 75	26.0	N4	+ 75	33.0
M5	+212	31.0	N5	+212	35.0
O6	-105	1.5	P2	-150	2.0
O2	- 62	4.0	P1	-125	1.0
O9	- 50	7.0	P11	-115	4.0
O10	- 37	3.0	P6	-105	27.0
O1	- 25	6.0	P8	- 75	22.0
O8	- 25	5.0	P9	- 50	36.0
O11	- 12	25.0	P10	- 25	44.0
O7	+ 3	26.0	P7	+ 3	70.0
O3	+ 32	37.0	P3	+ 32	66.0
O4	+ 75	44.0	P4	+ 75	63.0
O5	+212	43.0	P5	+212	67.0

Table 8. Charpy Test Results, Hot Work Samples
(Continued)

Code	Temperature (°F)	Energy (Ft-lb.)	Code	Temperature (°F)	Energy (Ft-lb.)
R11	-170	2.0	S6	-105	4.0
R2	-150	6.0	S2	-101	5.0
R1	-125	14.0	S1	- 94	7.0
R6	-105	26.0	S11	- 88	22.0
R10	- 88	30.0	S10	- 75	23.0
R8	- 75	32.0	S9	- 50	46.0
R9	- 50	57.0	S8	- 25	56.0
R7	+ 3	61.0	S7	+ 3	65.0
R3	+ 32	63.0	S3	+ 32	58.0
R4	+ 75	52.0	S4	+ 75	65.0
R5	+212	56.0	S5	+212	68.0
T6	-105	3.5	V6	-105	4.0
T2	- 88	10.0	V10	- 75	3.0
T10	- 75	7.0	V2	- 50	11.0
T1	- 62	5.0	V9	- 50	4.0
T11	- 62	10.5	V11	- 37	5.0
T9	- 50	23.0	V8	- 25	46.0
T8	- 25	37.0	V1	- 25	23.0
T7	+ 3	40.0	V7	+ 3	45.0
T3	+ 32	51.0	V3	+ 32	56.0
T4	+ 75	62.0	V4	+ 75	58.0
T5	+212	61.0	V5	+212	69.0

Table 9. Charpy Test Results,
Cold Work-Hot Work Samples

Code	Temperature (°F)	Energy (Ft-lb.)	Code	Temperature (°F)	Energy (Ft-lb.)
B7	-105	2.0	C6	- 50	2.0
B8	- 25	4.5	C5	- 25	2.0
B10	- 12	8.0	C7	+ 3	4.0
B11	0	4.0	C1	+ 17	3.0
B6	+ 3	24.0	C11	+ 25	6.0
B1	+ 17	20.0	C3	+ 32	15.0
B3	+ 32	16.0	C2	+ 55	17.0
B9	+ 55	22.0	C4	+ 75	15.0
B4	+ 75	28.0	C10	+ 87	27.5
B2	+150	44.0	C9	+100	25.0
B5	+212	38.0	C5	+212	25.0
D9	- 50	2.0	E6	-105	2.0
D8	- 25	3.0	E10	- 75	2.0
D7	+ 3	7.0	E9	- 50	2.0
D6	+ 32	11.0	E8	- 25	11.0
D1	+ 44	22.0	E2	- 12	8.0
D2	+ 55	23.0	E11	0	16.0
D11	+ 65	26.0	E7	+ 3	25.0
D4	+ 75	16.0	E1	+ 17	24.0
D10	+125	22.0	E3	+ 32	24.0
D5	+212	28.0	E4	+ 75	30.0
			E5	+212	43.0
F6	-105	2.0	G2	-150	2.0
F10	- 75	2.0	G1	-125	10.0
F9	- 50	4.0	G11	-115	14.0
F11	- 37	8.5	G6	-105	24.0
F8	- 25	22.0	G10	- 88	24.0
F1	- 12	36.0	G8	- 75	38.0
F2	- 12	29.0	G9	- 50	41.0
F7	+ 2	46.0	G7	+ 2	65.0
F3	+ 32	50.0	G3	+ 32	60.0
F4	+ 75	57.0	G4	+ 75	66.0
F5	+212	61.0	G5	+212	59.0

Table 9. Charpy Test Results,
Cold Work-Hot Work Samples
(Continued)

Code	Temperature (°F)	Energy (Ft-lb.)	Code	Temperature (°F)	Energy (Ft-lb.)
H2	-150	2.0	I6	-105	4.0
H1	-125	7.0	I11	- 88	13.0
H11	-115	6.0	I2	- 88	5.0
H6	-105	32.0	I10	- 75	23.0
H10	- 88	35.0	I1	- 62	24.0
H8	- 75	28.0	I9	- 50	37.0
H9	- 50	47.0	I8	- 25	51.0
H7	+ 3	73.0	I7	+ 3	51.0
H3	+ 32	66.0	I3	+ 32	52.0
H4	+ 75	72.0	I4	+ 75	60.0
H5	+212	75.0	I5	+212	61.0
J6	-105	3.0	K6	-105	4.0
J2	- 88	2.0	K10	- 75	2.5
J10	- 75	7.5	K2	- 62	10.0
J1	- 62	4.0	K9	- 50	34.0
J9	- 50	35.0	K11	- 37	3.0
J11	- 37	18.0	K8	- 25	26.0
J8	- 25	28.0	K1	- 12	20.0
J7	+ 3	37.0	K7	+ 3	35.0
J3	+ 32	48.0	K3	+ 32	41.0
J4	+ 75	53.0	K4	+ 75	58.0
J5	+212	60.0	K5	+212	64.0

Table 10. V-Notch Charpy Transition Temperature

Hot Work		Cold Work-Hot Work	
Code	15 Ft-lb. Transition (°F)	Code	15 Ft-lb. Transition (°F)
A	- 60	B	+ 22
L	+ 65	C	+ 55
M	+ 20	D	+ 40
N	- 15	E	- 2
O	- 20	F	- 30
P	-100	G	-115
R	-129	H	-105
S	- 87	I	- 80
T	- 60	J	- 42
V	- 37	K	- 37

Table 11. Hardness Test Results,
Hot Work Samples

Code	Finishing Temperature °F	Rockwell B	Rockwell C	Brinnell 3000 Kp. 10 mm Ball
A	Mill	85	---	158
L	800	---	25	265
M	950	100	19	235
N	1100	98	16	225
O	1250	95	---	205
P	1400	91	---	185
R	1550	82	---	148
S	1700	84	---	155
T	1850	85	---	158
V	2000	88	---	170

Table 12. Hardness Test Results,
Cold Work-Hot Work Samples

Code	Finishing Temperature °F	Rockwell B	Rockwell C	Brinnell 3000 Kp. 10 mm Ball
B	Cold Rolled	94	---	195
C	800	---	25	265
D	950	---	23	245
E	1100	---	17	215
F	1250	90	---	185
G	1400	89	---	175
H	1550	88	---	170
I	1700	84	---	155
J	1850	86	---	160
K	2000	88	---	170

Table 13. Optical Metallographic Results,
Hot Work Samples

Code	Finishing Temperature (°F)	Magnifi- cation	Ferrite Mean Intercept (d) (in $\times 10^4$)	$d^{-\frac{1}{2}}$ (in $^{-\frac{1}{2}}$)	Pearlite %	Ferrite Orientation Factor %
A	M111	200x	7.6	36.2	31.7	10
A	M111	200x	8.0	35.3	29.4	15
A	M111	200x	8.0	35.3	24.6	14
A	M111	400x	5.2	43.6	34.5	5
L	800	200x	7.5	36.6	23.4	46
L	800	400x	6.0	40.7	31.3	42
L	800	400x	5.5	42.7	28.6	44
M	950	200x	9.4	32.5	21.8	39
M	950	400x	6.2	40.3	28.2	42
M	950	400x	6.1	40.4	26.2	44
N	1100	200x	8.6	34.0	30.2	40
N	1100	400x	5.8	41.4	29.4	42
N	1100	400x	6.3	39.8	22.2	42
O	1250	200x	7.6	36.3	30.6	50
O	1250	400x	5.6	42.1	32.9	48
O	1250	400x	5.6	42.1	33.3	46
P	1400	400x	3.2	56.2	24.6	22
R	1550	400x	3.5	53.4	29.8	8
R	1550	400x	3.2	56.2	30.6	19
S	1700	200x	7.0	37.8	30.2	12
S	1700	200x	7.2	37.1	33.7	13
T	1850	200x	6.0	40.7	27.8	7
T	1850	200x	6.3	39.9	31.7	9
V	2000	200x	7.2	37.3	29.0	8
V	2000	200x	6.6	38.9	30.2	12

Table 14. Optical Metallographic Results,
Cold Work-Hot Work Samples

Code	Finishing Temperature (°F)	Magnifi- cation	Ferrite Mean Intercept (d) (in x 10 ⁴)	$d^{-\frac{1}{2}}$ (in ^{-$\frac{1}{2}$})	Pearlite %	Ferrite Orientation Factor %
B	Cold Rolled	200x	8.0	35.3	26.2	29
B	Cold Rolled	200x	7.7	36.0	28.6	29
C	800	200x	7.1	37.4	29.0	38
C	800	200x	7.3	37.0	27.8	40
D	950	200x	6.5	39.1	36.1	38
D	950	400x	5.3	43.6	30.9	43
D	950	400x	5.3	43.3	37.3	48
E	1100	200x	7.1	37.5	35.7	32
E	1100	200x	8.0	35.3	34.9	36
F	1250	200x	7.8	35.9	29.4	39
F	1250	200x	8.4	34.5	29.4	43
G	1400	400x	3.0	57.4	23.4	22
G	1400	400x	3.2	55.8	23.8	21
H	1550	400x	2.9	58.5	34.9	7
H	1550	400x	3.2	55.8	33.3	19
I	1700	200x	6.7	38.7	35.3	12
I	1700	400x	4.5	46.9	34.5	13
I	1700	400x	5.0	45.2	34.9	7
J	1850	200x	7.9	35.6	29.4	4
J	1850	200x	7.9	35.6	30.4	14
K	2000	200x	7.5	36.5	32.9	12
K	2000	200x	7.4	36.9	36.1	16

CHAPTER V

CONCLUSIONS AND DISCUSSIONS

"Hot Work" Code Designation

If calculated values of mechanical properties and the results of quantitative metallographic examinations are plotted against a significant variable, as the temperature at which the steel enters the rolling mill, then a number of conclusions become immediately apparent:

1. There is a strong influence on values of yield strength when fabrication temperatures are decreased below the 1400-1550°F range, the yield strength values strongly increasing with decreasing temperature at the mill, as Figures 3 and 5 show.
2. Variations of yield strength values resulting from variations of fabrication temperatures, when the temperatures are above 1400-1550°F are reduced, as compared with Conclusion One above, as shown by Figures 3 and 5.
3. The Hall-Petch equation appears to be applicable when fabrication temperatures are in excess of 1400°F, as indicated by Figure 4. The applicable formulation is

$$\sigma_y = 39,800 + 350d^{-\frac{1}{2}} \quad (23)$$

4. Values of the strain hardening exponent n strongly decrease with decreasing fabrication temperatures below 1400°F (Figure 6).
5. Values of the strength coefficient K strongly increase with decreasing fabrication temperatures below 1250°F , as shown by Figure 7: in fact, there indeed may be a minimum for fabrication temperatures near 1250°F (Figure 8).
6. Measures of ductility, as the percent elongation, strongly decrease at fabrication temperatures below 1400°F (Figures 9 and 10).
7. There is a minimum of 15 foot pound ductile-brittle transition temperature, as determined by V-notch Charpy specimens, associated with fabrication in the 1400 - 1700°F range, as shown by Figure 11.
8. The orientation factor abruptly changes values when fabrication temperatures are lowered below 1250°F , the values of the orientation factor being practically constant for higher fabrication temperatures, as shown by Figure 12.

An inescapable conclusion is that abrupt changes of many properties result with A-441 steel when fabrication temperatures are dropped below 1400°F . In fact, for a structural steel such as A-441 the combination of properties resulting from 1550°F fabrication are outstanding -- ductility is at a maximum (Figures 9 and 10); measures of resistance to deformation are good, yield and ultimate strength values

being in excess of those obtained for the production mill finished sample designated as A (Tables 2, 4); the 15 foot pound Charpy ductile-brittle transition temperature is outstanding (Table 10).

There must be a unique feature associated with fabrication near a temperature of 1550°F. This temperature would be near the expected austenite-ferrite transformation A_3 line for the steel under consideration, although the rapid cooling associated with mill entry would probably suppress the transformation temperature. It is concluded that at about 1400-1550°F mill entry temperature fabrication is being accomplished which strengthens austenite; the fabrication is probably simultaneous with carbide, nitride, or carbonitride precipitation. Thus, high temperature thermomechanical treatment (HTTMT) with unusually rewarding effects have been accomplished.

When fabrication is accomplished at temperatures below about 1400°F there are large increases of the friction stress, explaining the departure from linearity shown by Figure 4 at the lower fabrication temperatures. This concept is completely consistent with behavior illustrated by Figures 3, 5, 6, 7, and 8. At the lower temperatures the fabrication may be simultaneous with aging, resulting in the unusually high transformation temperatures shown by Figure 11. Cold work effects must persist after fabricating at temperatures approaching the A_1 line.

A further study of microstructures verifies the conclusions and postulations made here, as a comparison of the 400x microstructures of samples T, R, P, and O shown by Figure 13 indicate. Values of pearlite mean intercept include the following for the four samples: T, 5.20×10^{-4}

inch, R, 3.25×10^{-4} inch; P, 2.18×10^{-4} inch; and O, 5.08×10^{-4} inch. It is apparent that the pearlite has become more disperse in the ferrite matrix at the fabrication temperatures giving optimum combinations of properties. One expected result would be increased toughness and ductility, as shown by the "R" material.

"Cold Work-Hot Work" Code Designation

A comparison of the results shown by Figures 14 through 23, obtained with samples coded C, D, E, F, G, H, I, J, and K with the previously discussed results shown by Figures 3 and 13, obtained with the "hot work" samples coded L, M, N, O, P, R, S, T, and V will show that there are, at the most, minimal differences between equivalent Figures. It must be concluded that the preliminary thermomechanical treatment (PTMT) as practiced here is ineffective. The effects of initial cold work, before the elevated temperature fabrication, are completely done away with, either in the furnace, through recrystallization, or by a combination of thermal and processing effects.

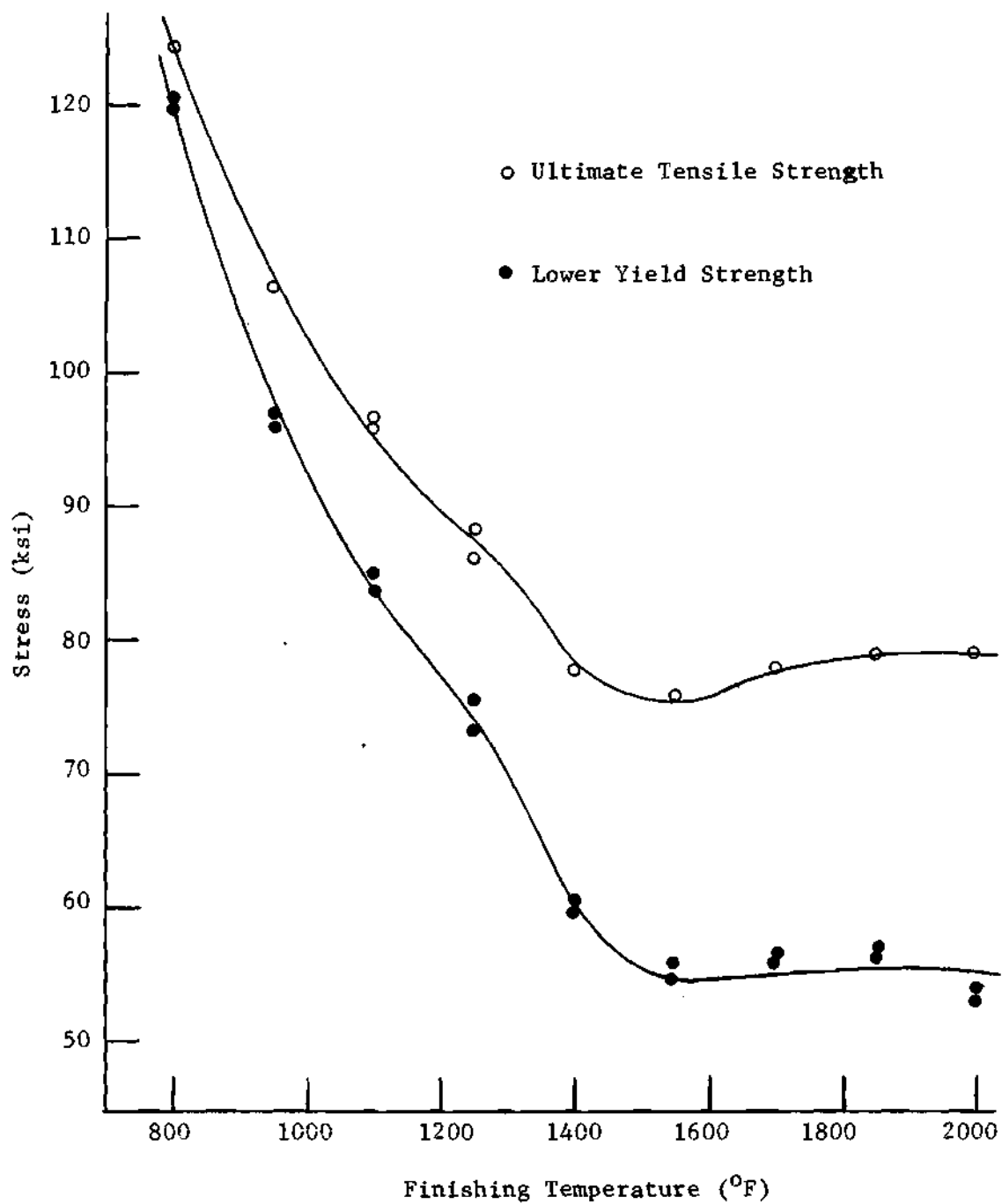


Figure 3. Yield Strength and Ultimate Tensile Strength as Functions of Fabrication Temperature, Hot Work Longitudinal Specimens

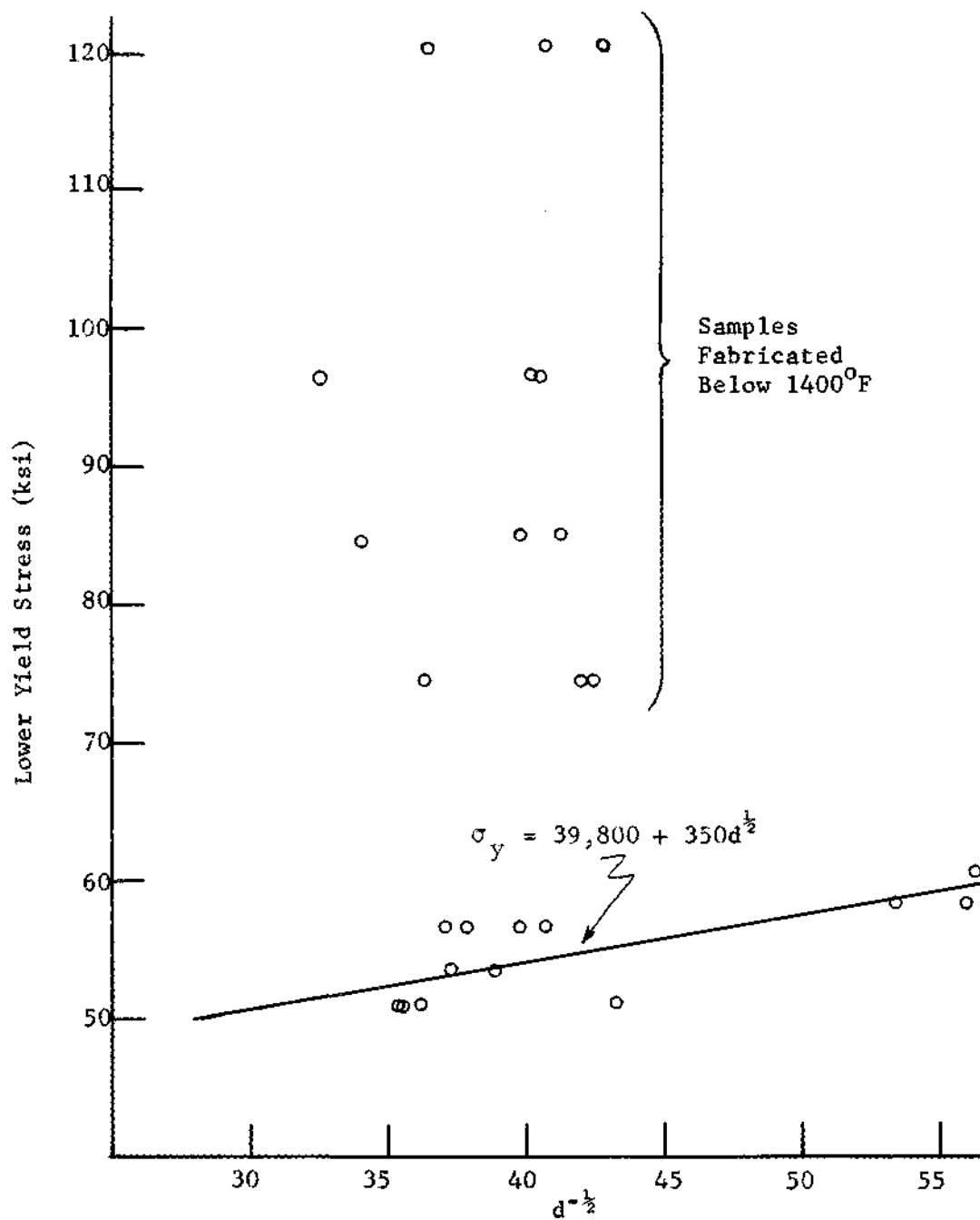


Figure 4. Applicability of Hall-Petch Equation for High Temperature Fabricated A-441, Hot Work Longitudinal Specimens

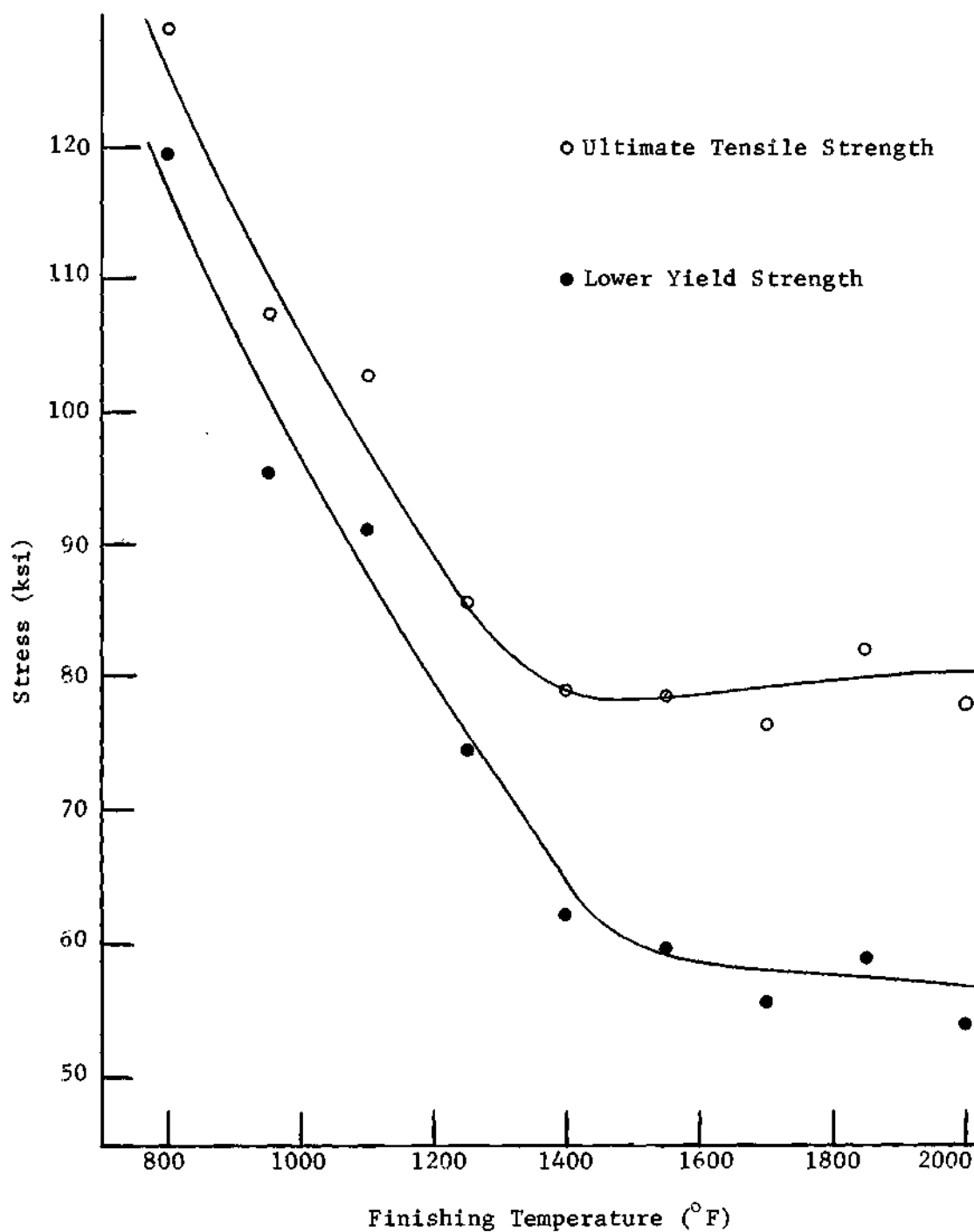


Figure 5. Yield Strength and Ultimate Tensile Strength as Functions of Fabrication Temperature, Hot Work Transverse Specimens.

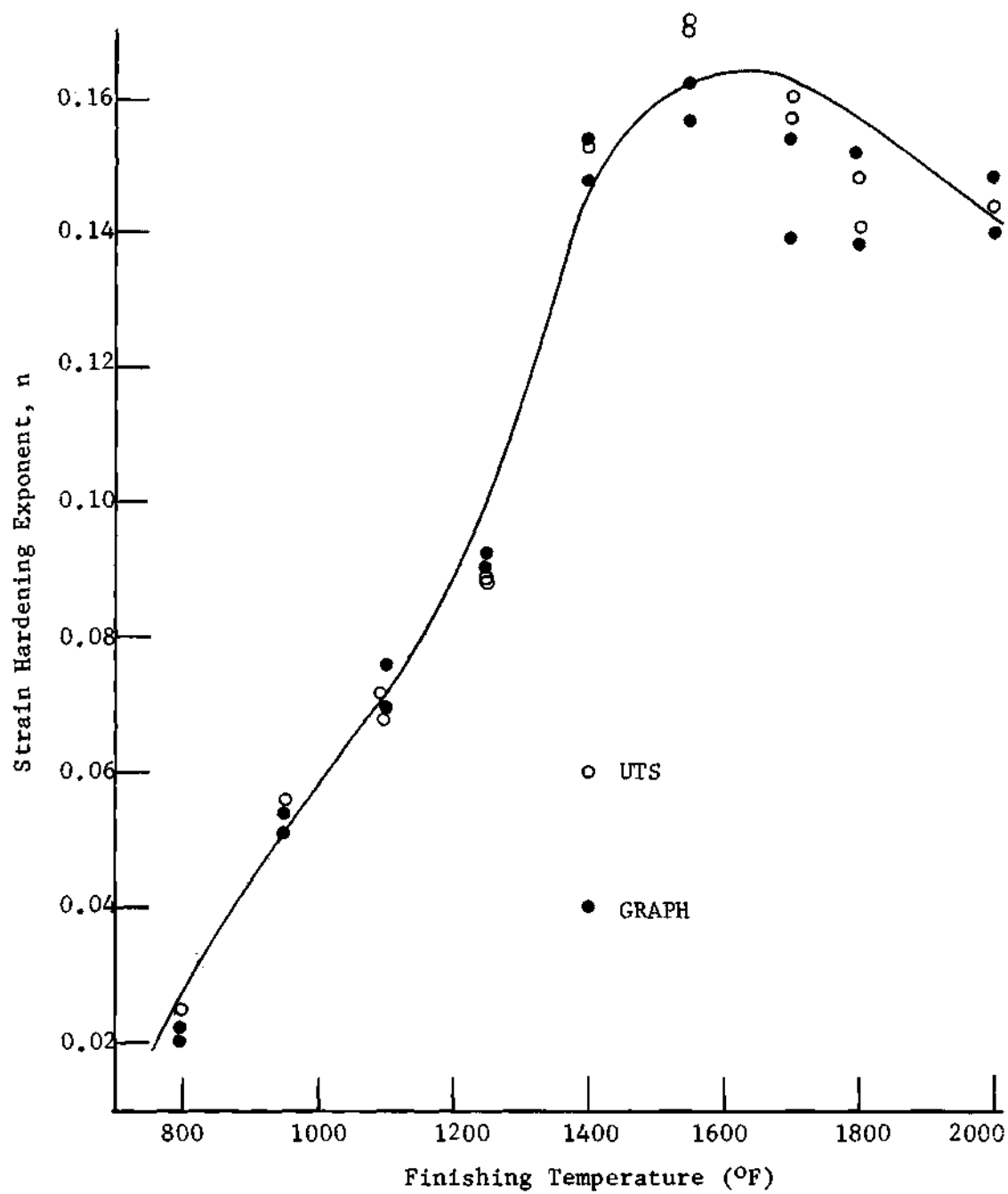


Figure 6. Strain Hardening Exponent as a Function of
Fabrication Temperature, Hot Work Longitudinal
Specimens

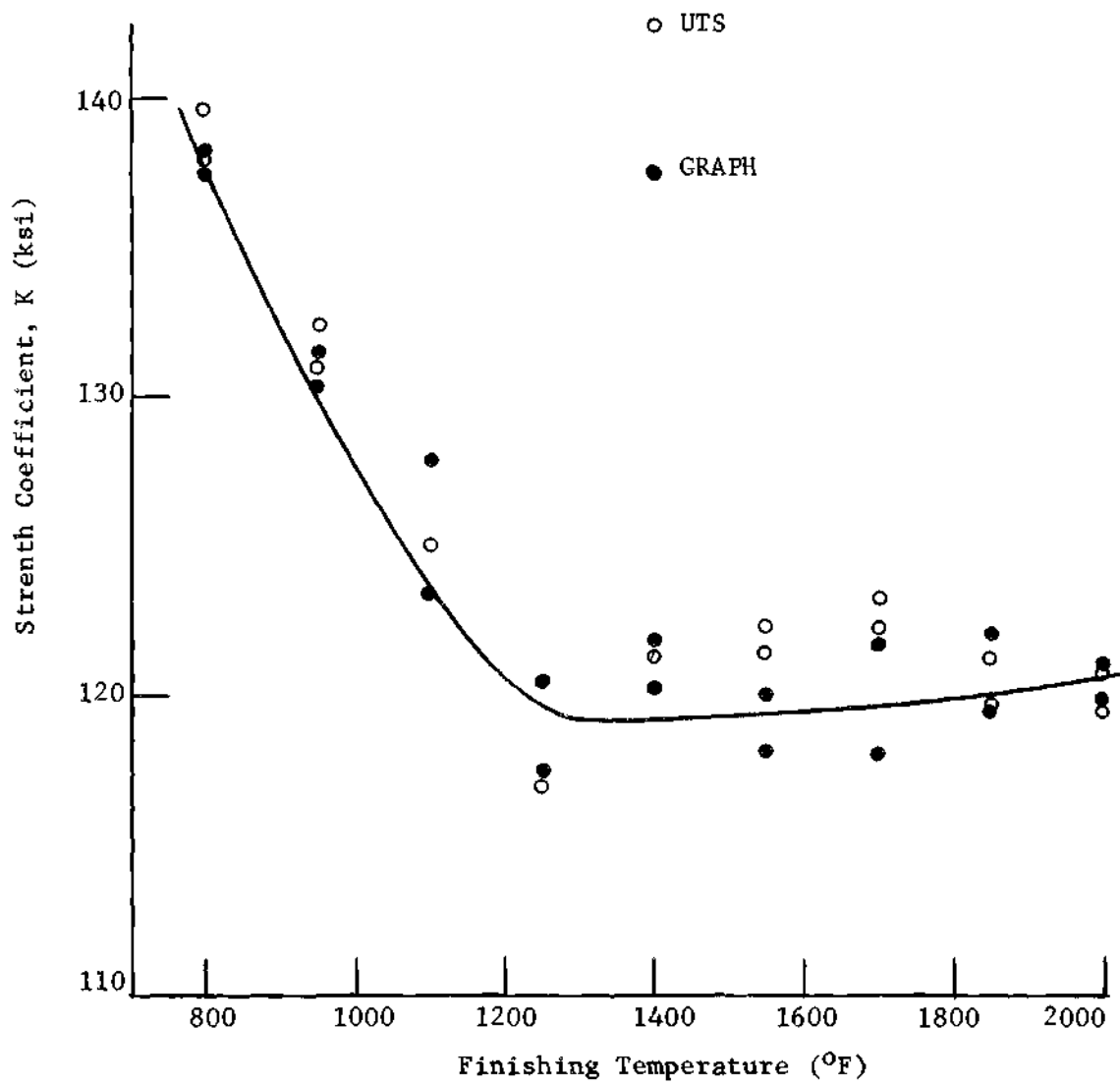


Figure 7. Strength Coefficient as a Function of
Fabrication Temperature, Hot Work
Longitudinal Specimens

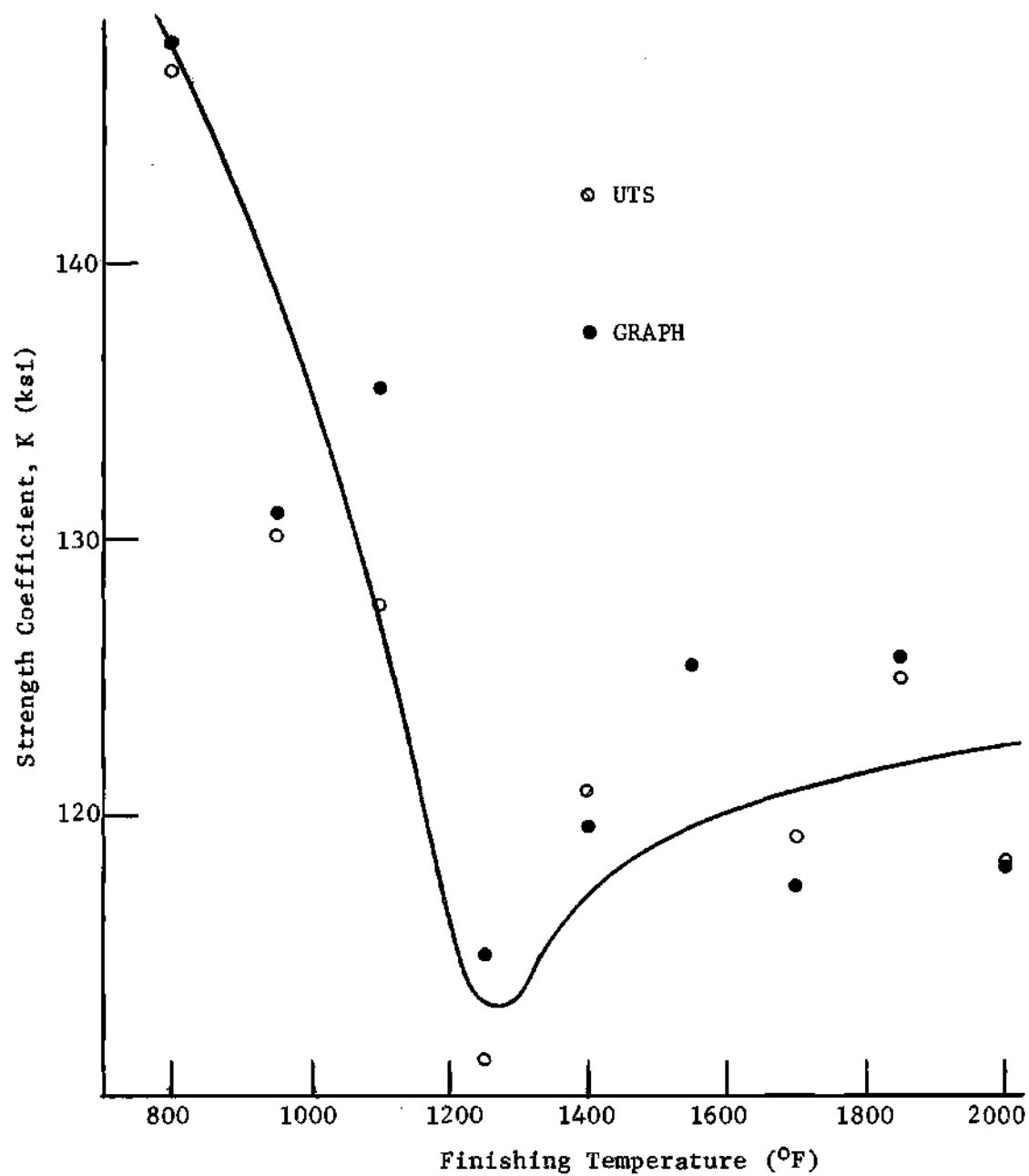


Figure 8. Strength Coefficient as a Function of
Fabrication Temperature, Hot Work Transverse
Specimens

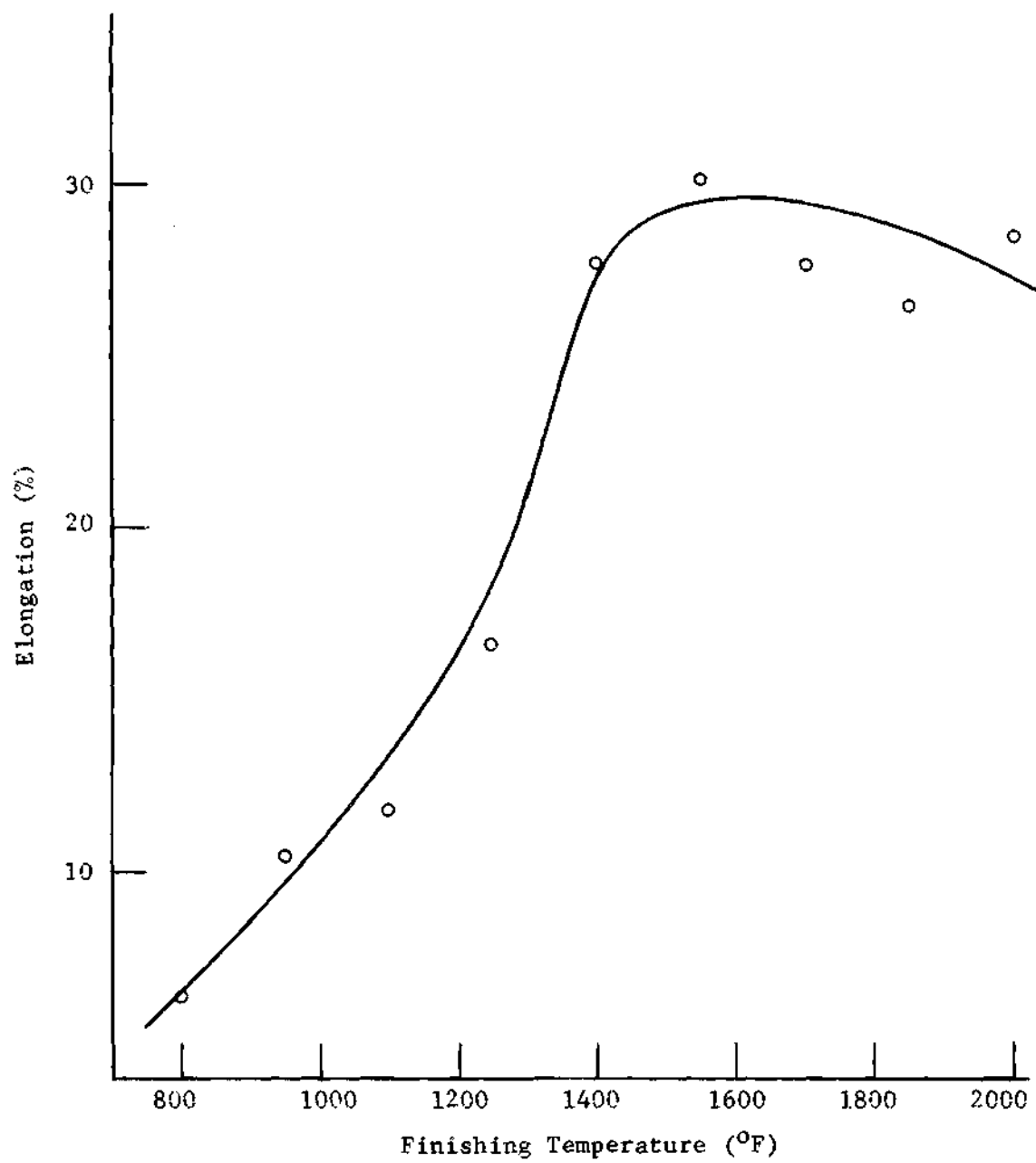


Figure 9. Percent Elongation as a Function of
Fabrication Temperature, Hot Work
Transverse Specimens

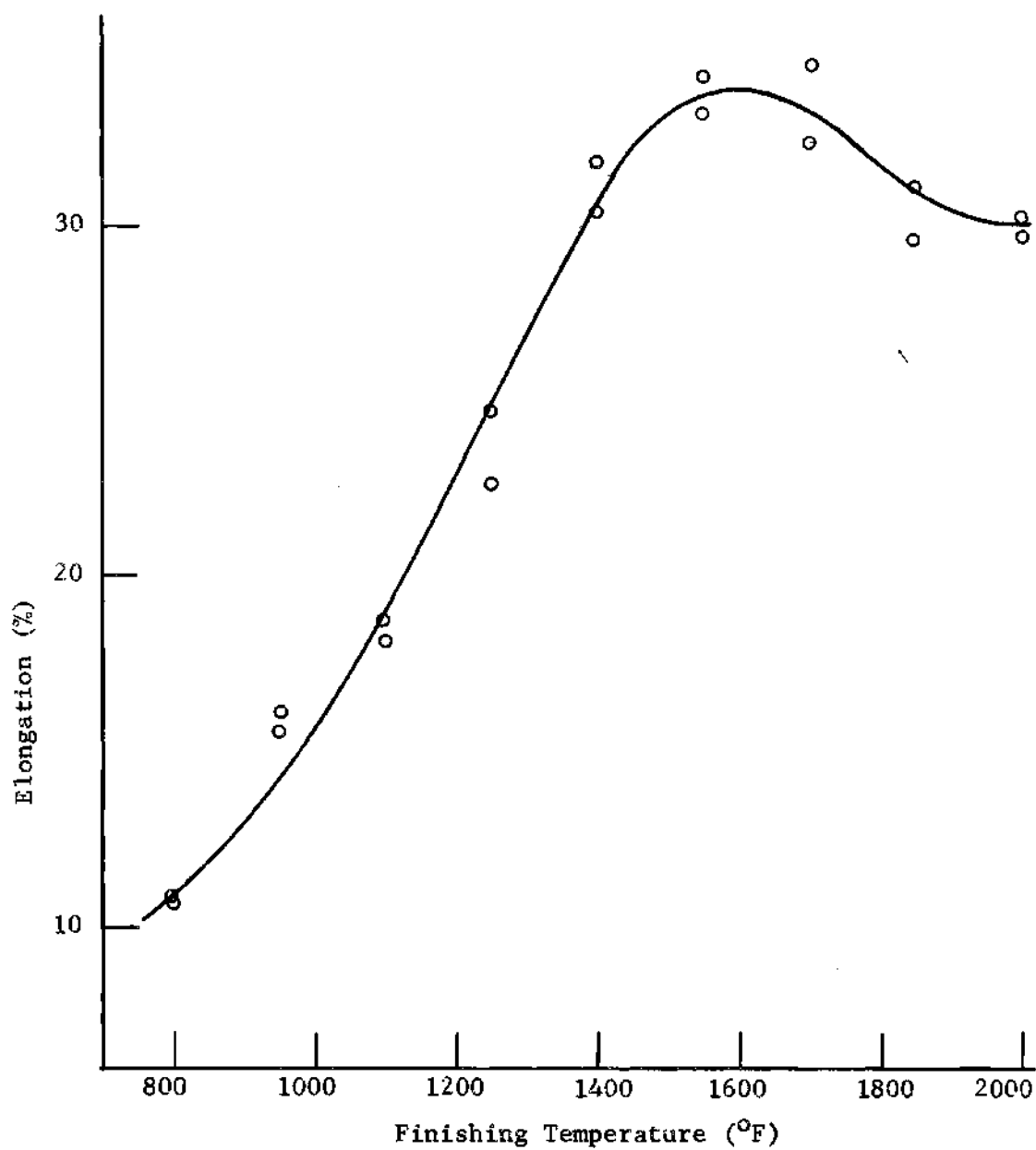


Figure 10. Percent Elongation as a Function of
Fabrication Temperature, Hot Work
Longitudinal Specimens

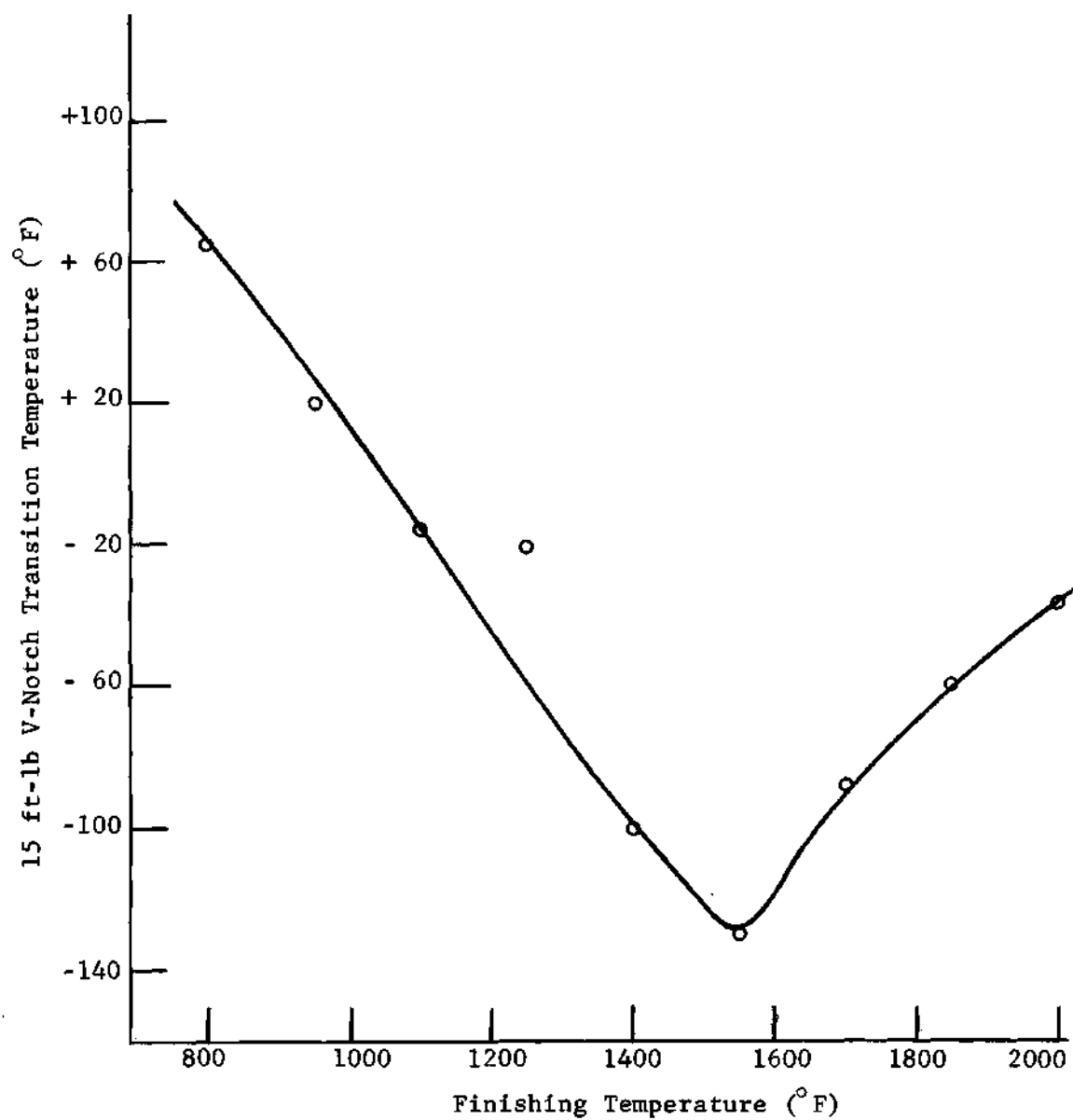


Figure 11. V-Notch Transition Temperature as a Function of
Fabrication Temperature, Hot Work Specimens

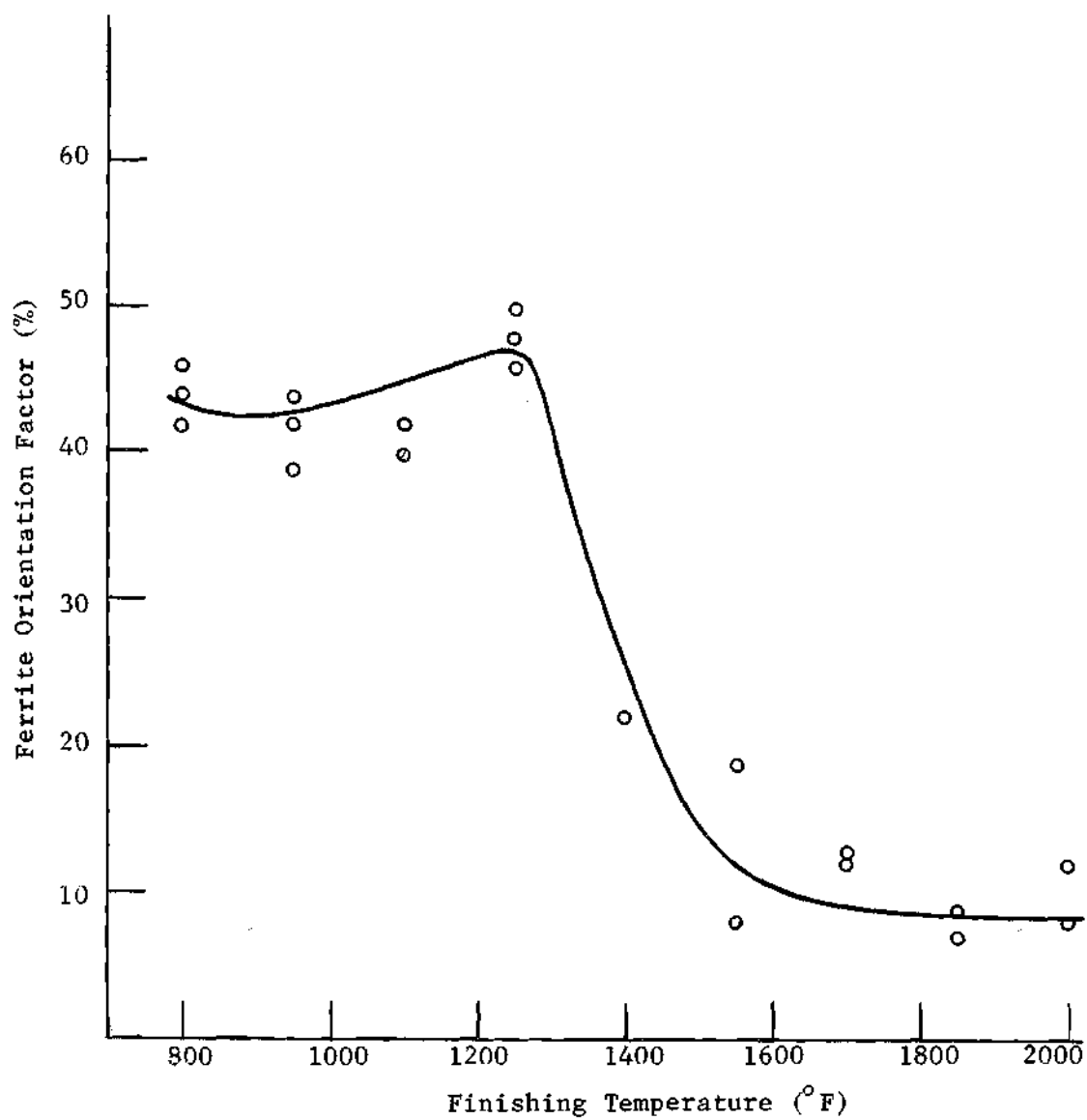


Figure 12. Ferrite Orientation Factor as a Function of
Fabrication Temperature, Hot Work Specimens



(a) Specimen 0, Fabricated at 1250°F,
Magnification 400x

Figure 13. Photomicrographs, Hot Work Samples



(b) Specimen P, Fabricated at 1400°F,
Magnification 400x

Figure 13. Photomicrographs, Hot Work Samples (Continued)



(c) Specimen R, Fabricated at 1550° F,
Magnification 400x

Figure 13. Photomicrograph, Hot Work Samples (Continued)



(d) Specimen T, Fabricated at 1850°F,
Magnification 400x

Figure 13. Photomicrograph, Hot Work Samples (Continued)

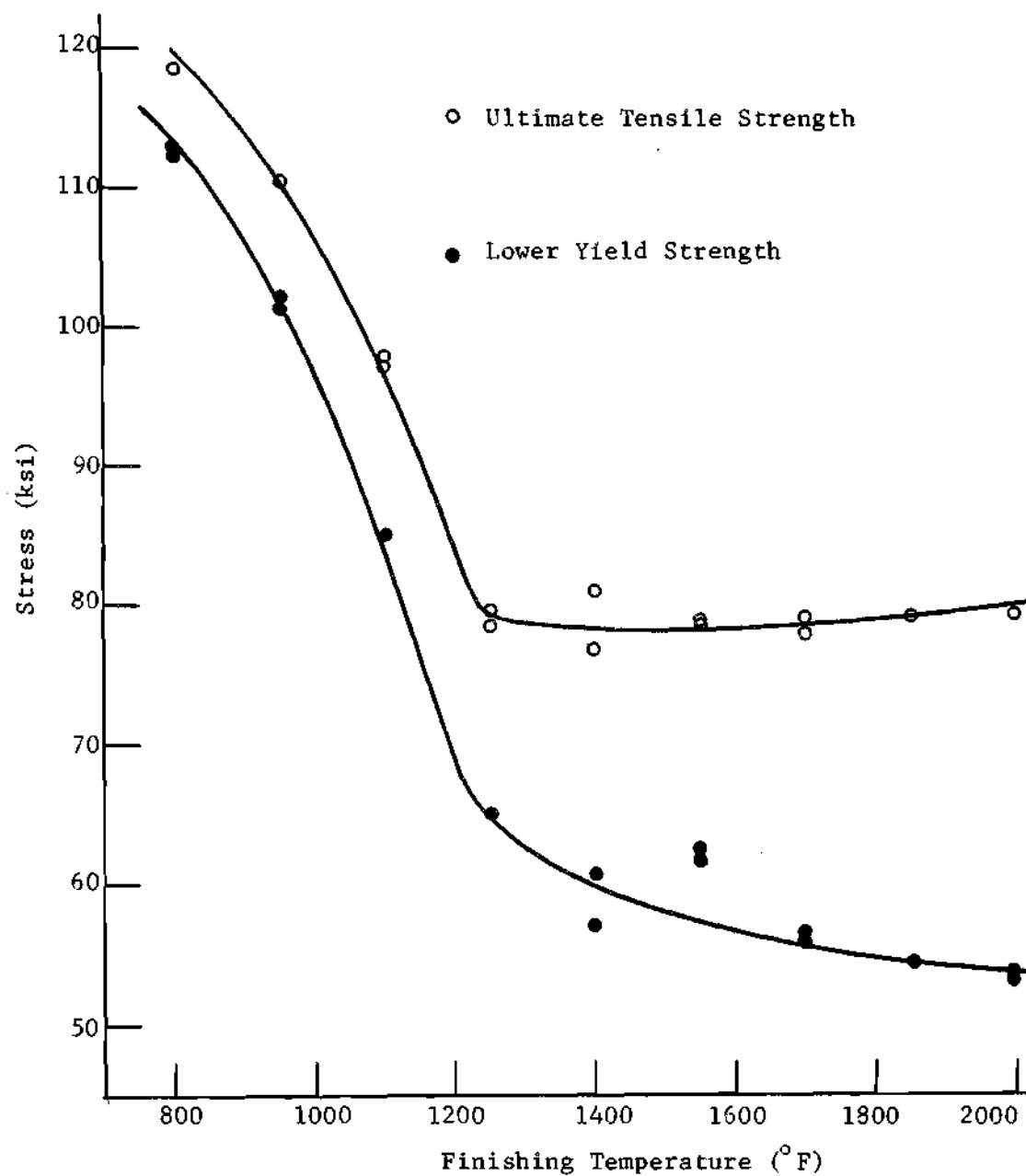


Figure 14. Yield Strength and Ultimate Tensile Strength as Functions of Fabrication Temperature, Cold Work-Hot Work Longitudinal Specimens

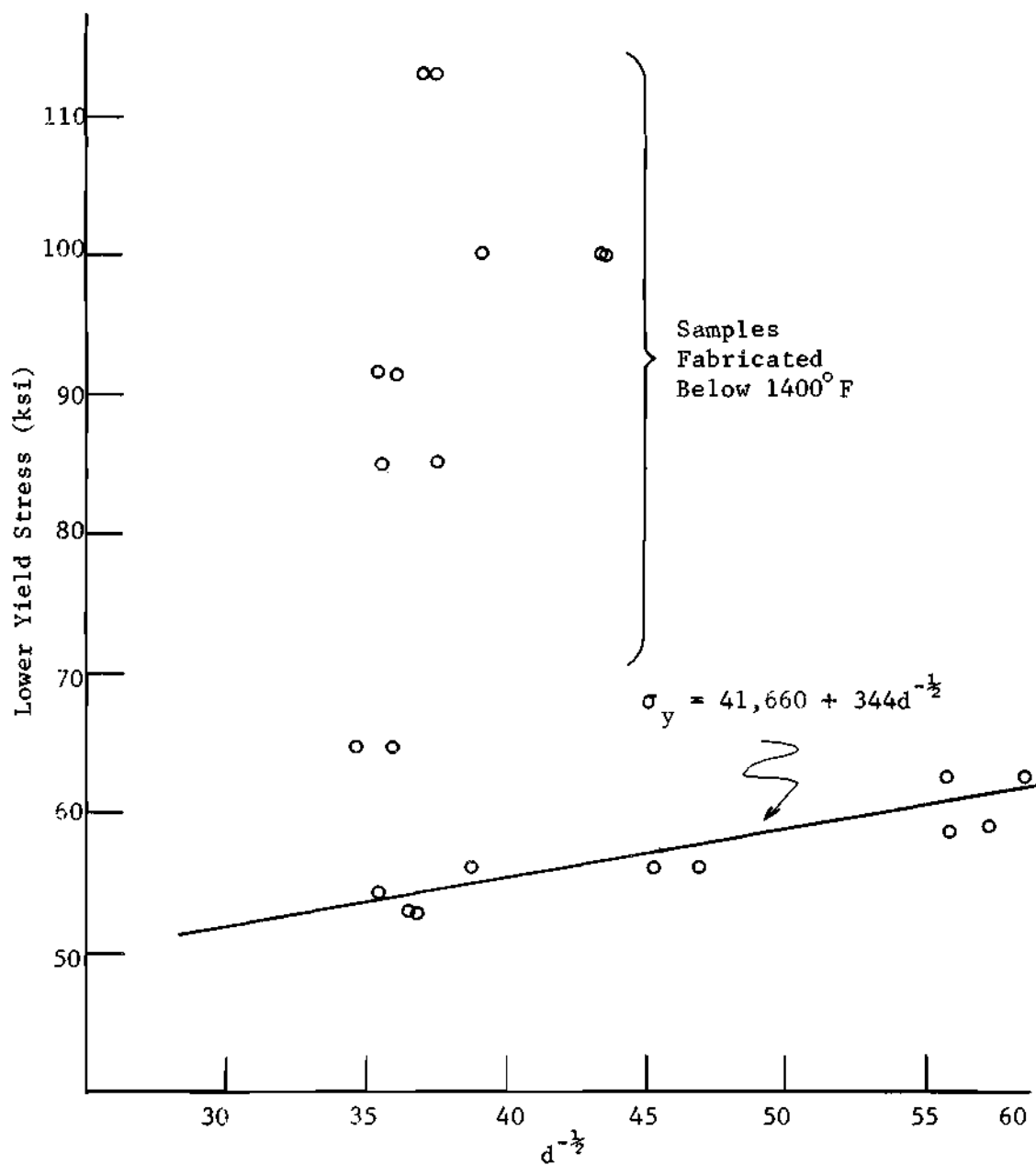


Figure 15. Applicability of Hall-Petch Equation for High Temperature Fabricated A-441, Cold Work-Hot Work Longitudinal Specimens

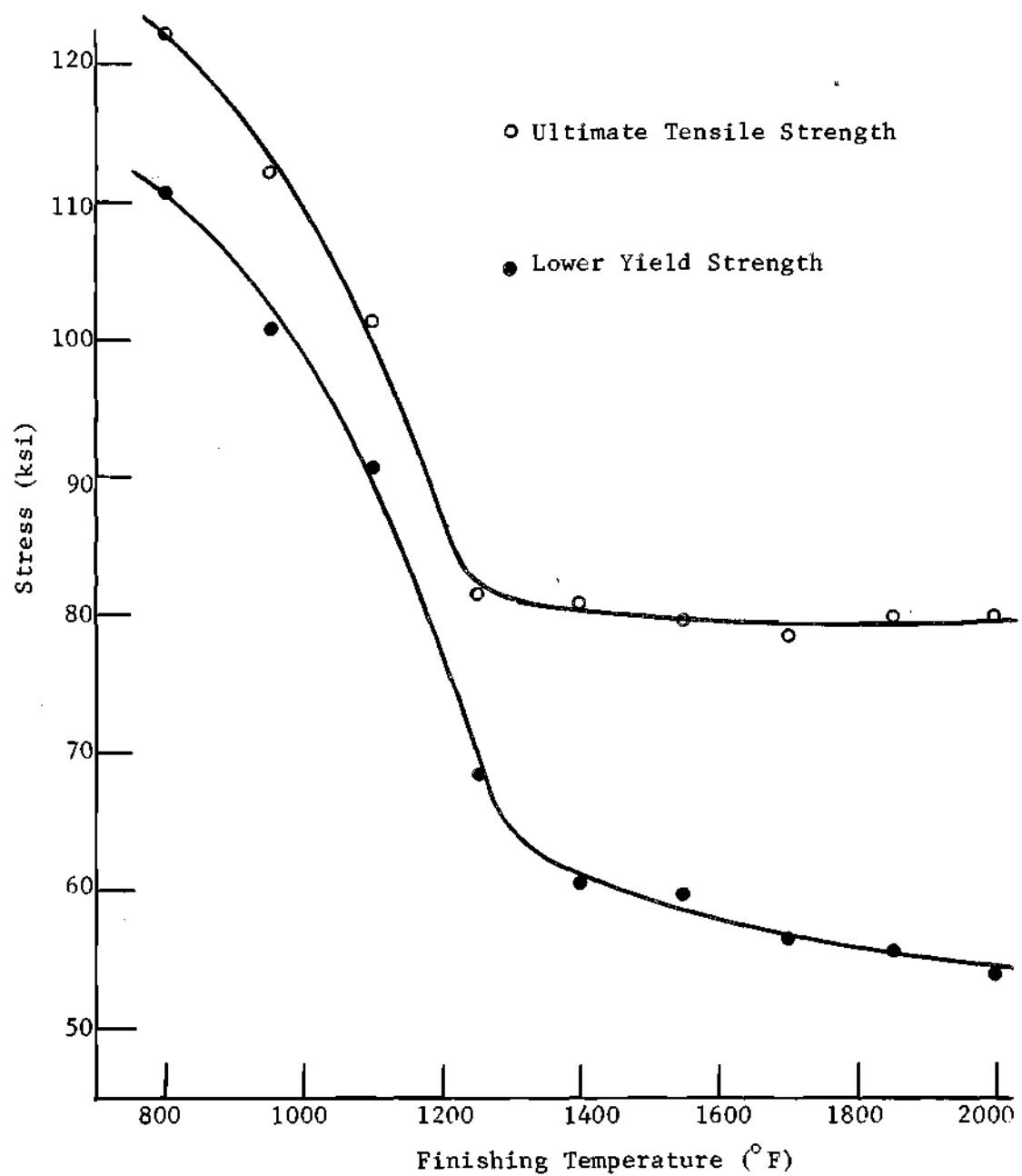


Figure 16. Yield Strength and Ultimate Tensile Strength as Functions of Fabrication Temperature, Cold Work-Hot Work Transverse Specimens

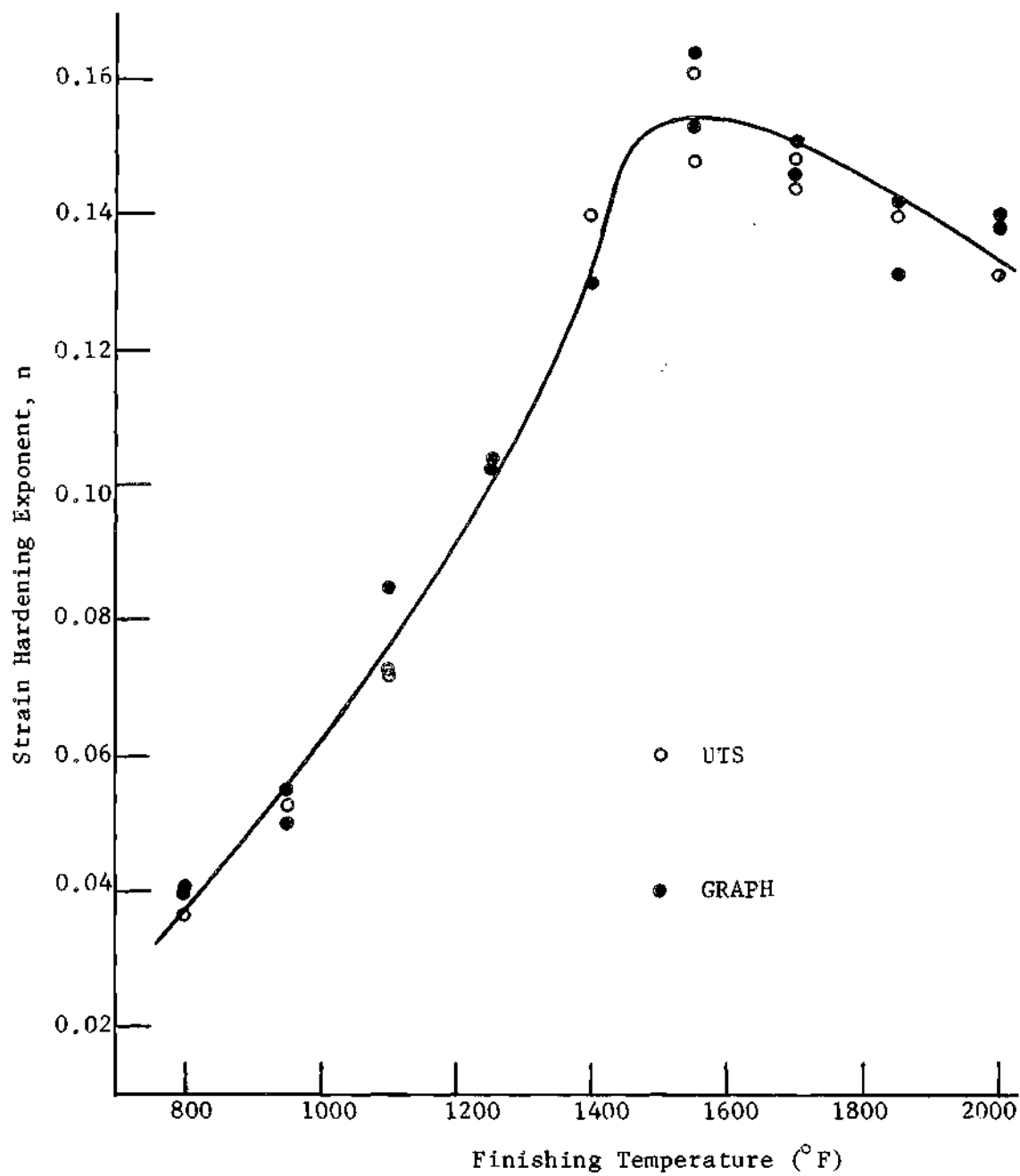


Figure 17. Strain Hardening Exponent as a Function of
Fabrication Temperature, Cold Work-Hot Work
Longitudinal Specimens

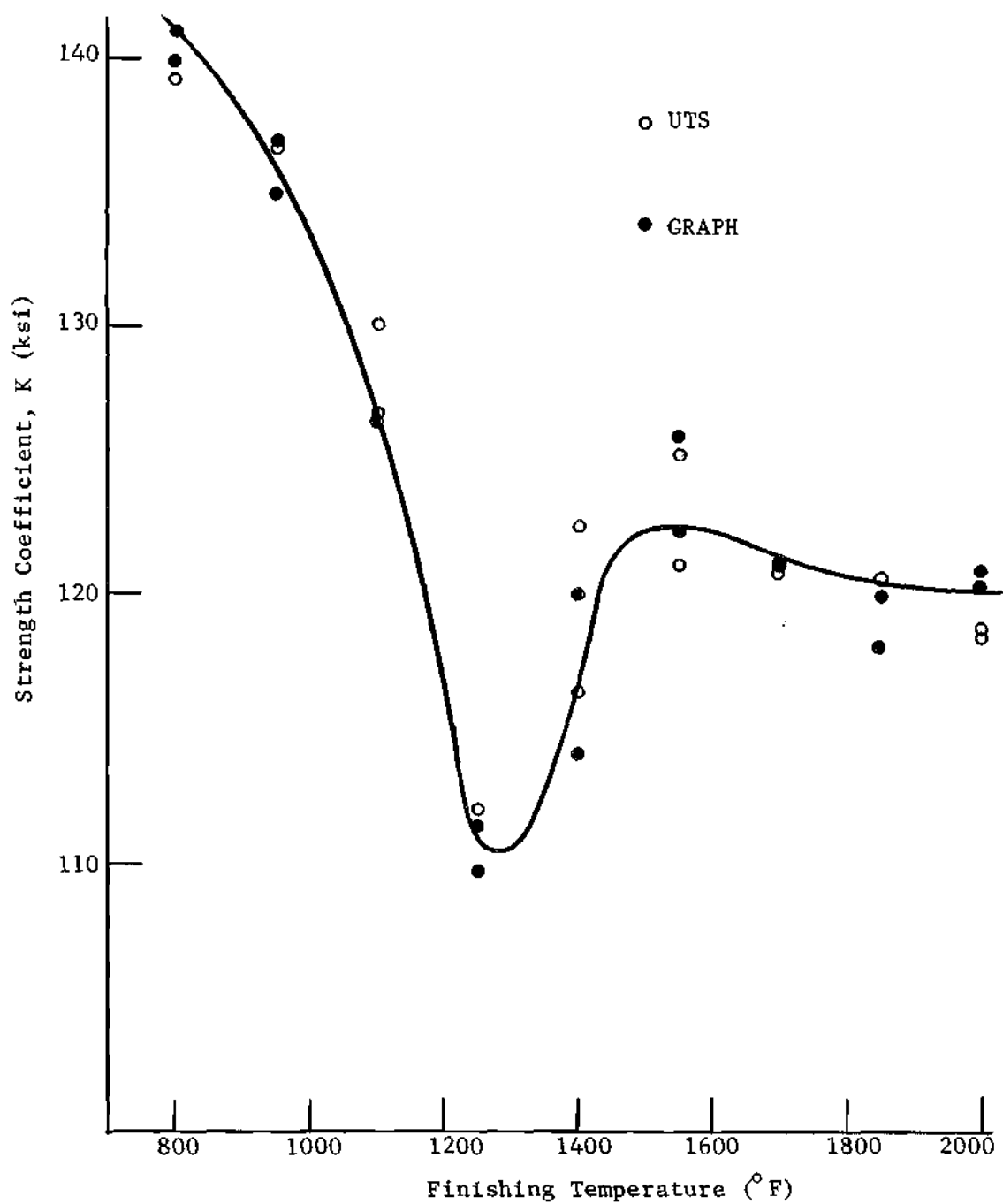


Figure 18. Strength Coefficient as a Function of Fabrication Temperature, Cold Work-Hot Work Longitudinal Specimens

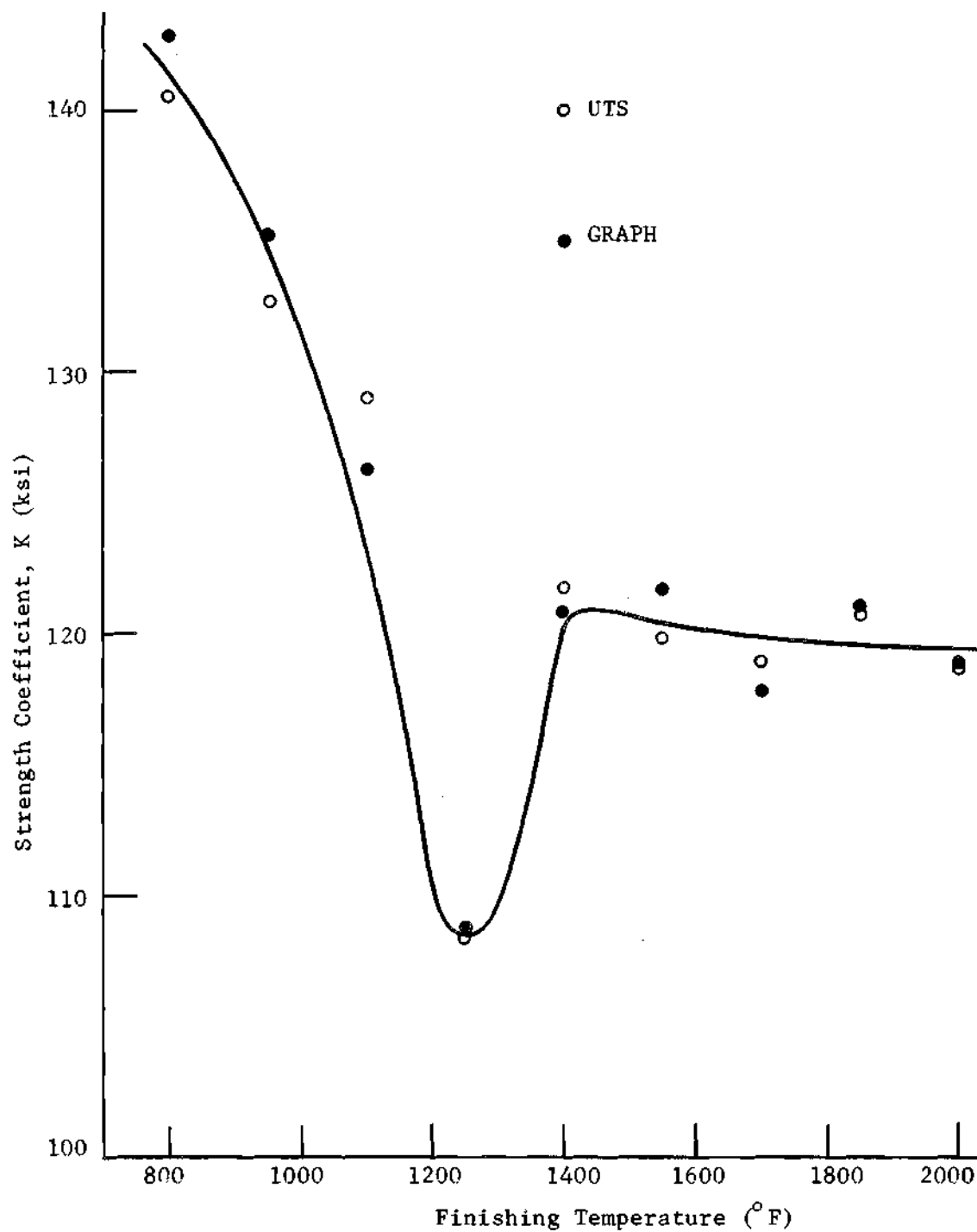


Figure 19. Strength Coefficient as a Function of Fabrication Temperature, Cold Work-Hot Work Transverse Specimens

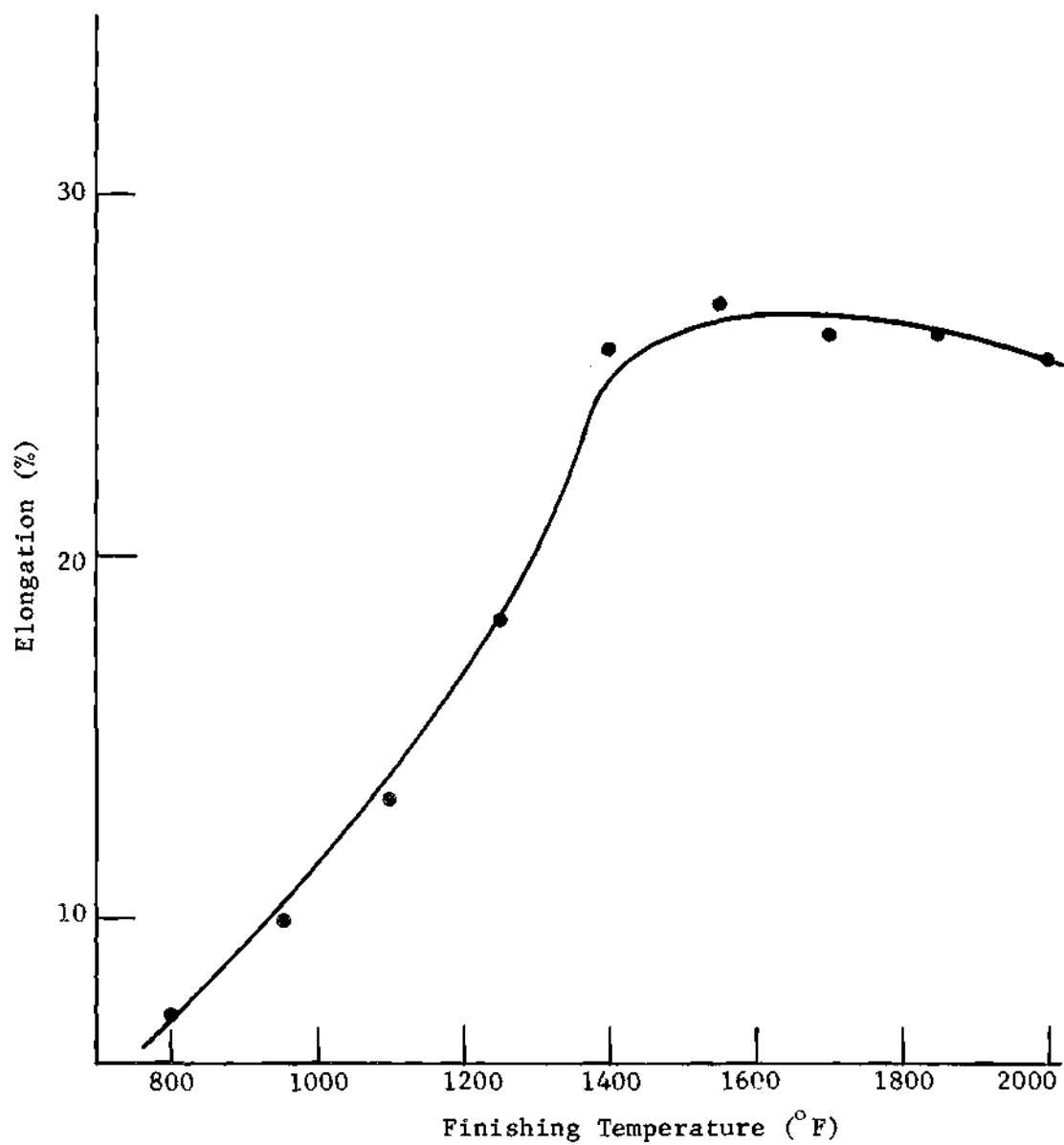


Figure 20. Percent Elongation as a Function of Fabrication Temperature, Cold Work-Hot Work Specimens

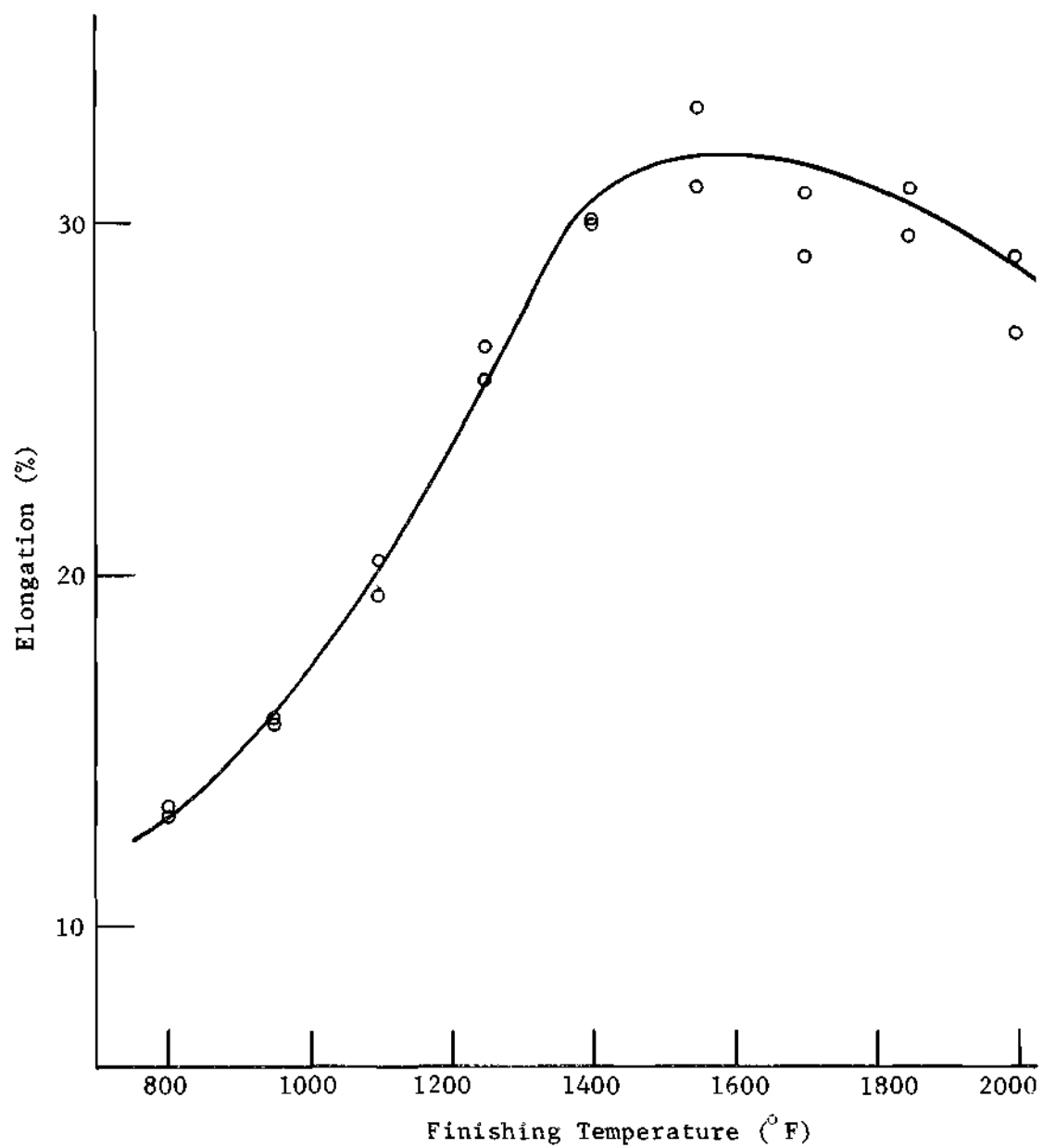


Figure 21. Percent Elongation as a Function of Fabrication Temperature, Cold Work - Hot Work Transverse Specimens

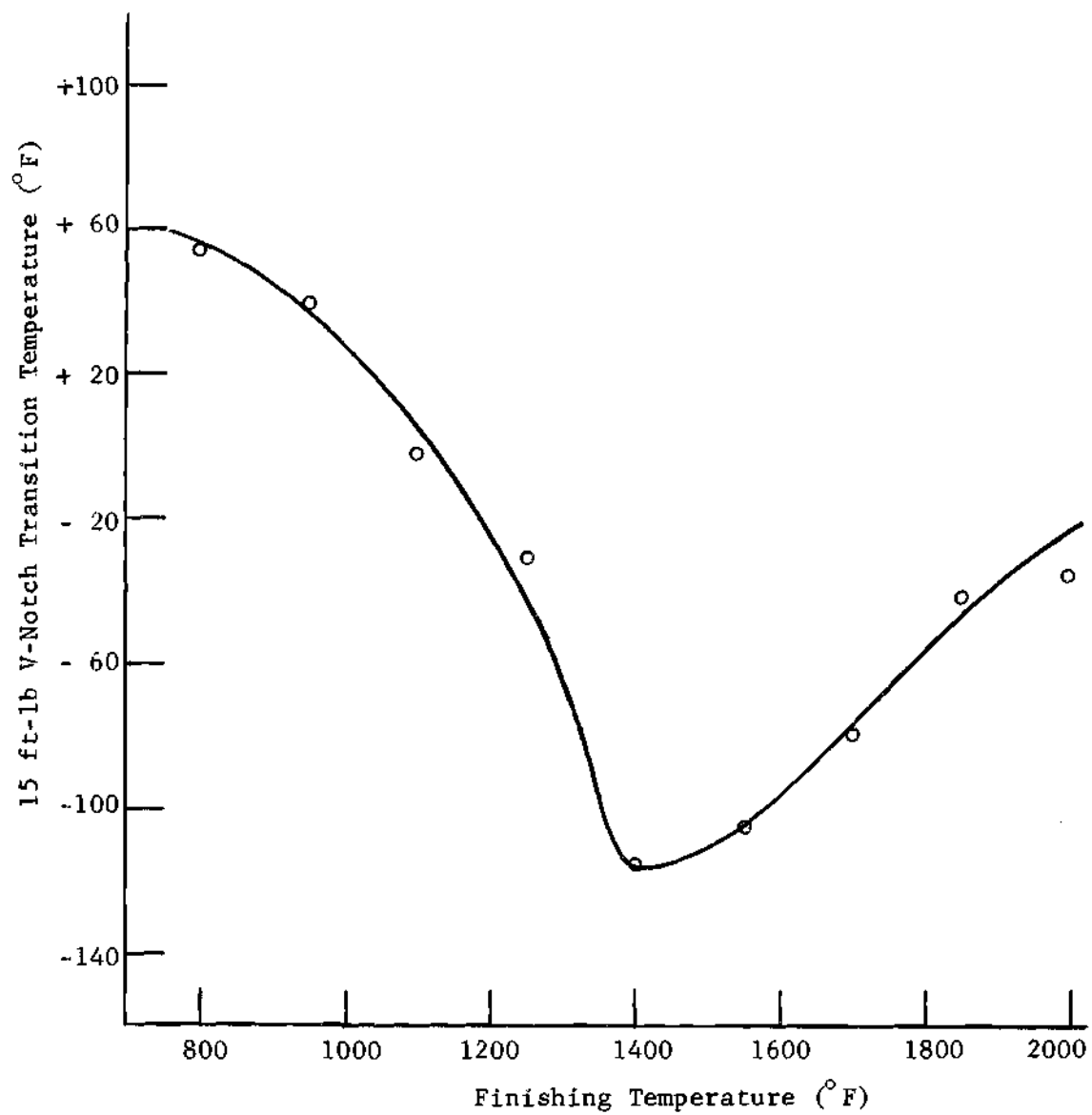


Figure 22. V-Notch Transition Temperature as a Function of
Fabrication Temperature, Cold Work-Hot Work
Specimens

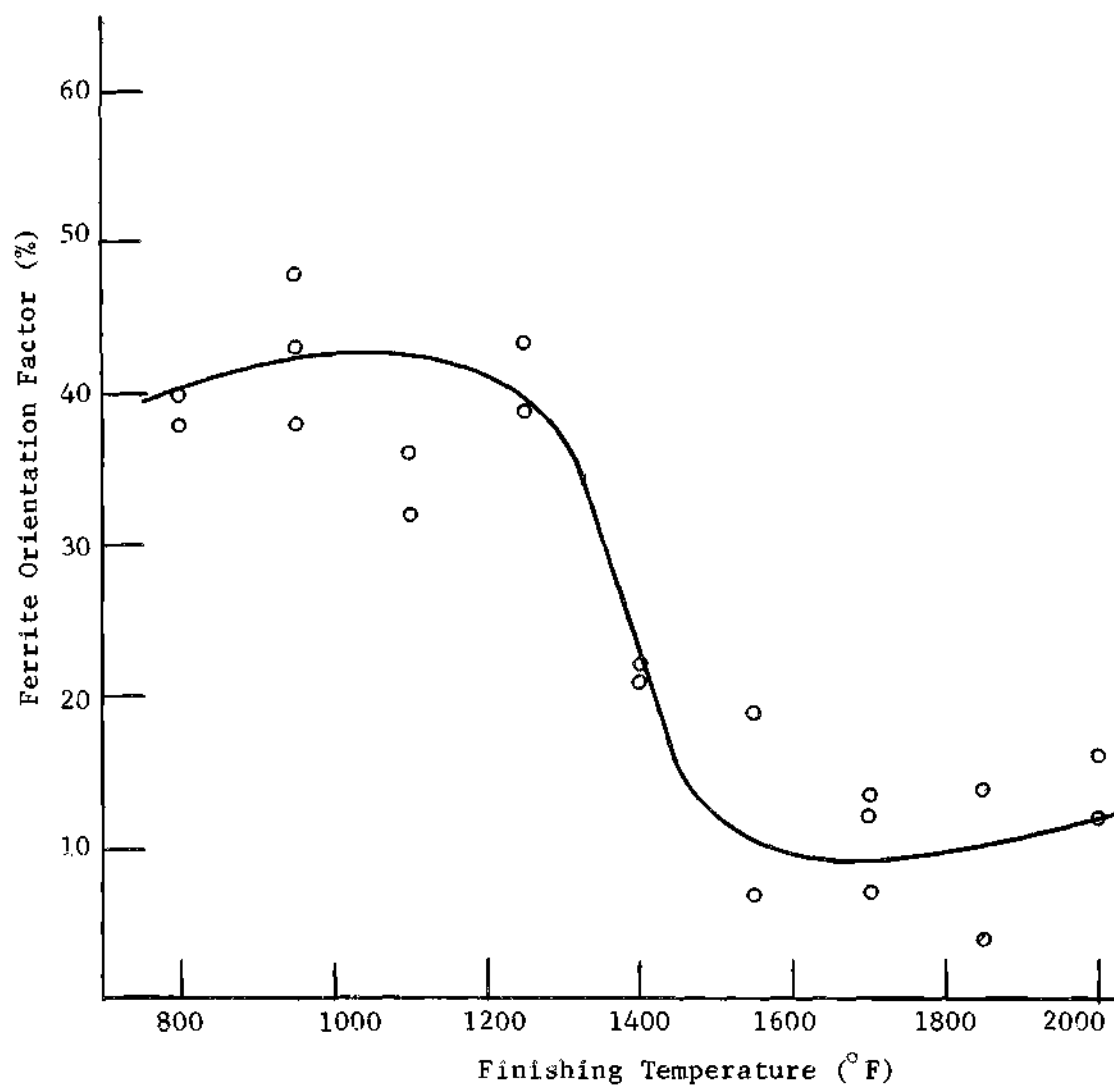


Figure 23. Ferrite Orientation Factor as a Function of
Fabrication Temperature, Cold Work - Hot Work
Specimens

CHAPTER VI

RECOMMENDATIONS

As a result of this thesis there are now available a total of 18 samples of A-441 which have received different thermomechanical treatments; there are also two control samples representative of mill finished and cold worked A-441, respectively. Work which could be easily accomplished at the electron microscope, by a competent engineer or scientist, could greatly help the explanation of observed effects, particularly as regards precipitation and cold work effects. Further work having to do with the state of aging of the material fabricated in the 800-1100°F range would also be expected to be rewarding.

BIBLIOGRAPHY

1. Anonymous, "Compositions, Properties, and Producers of High Strength Steel," Metal Progress, Vol. 92, pp 87, 1965.
2. Yeo, R. B. G., A. G. Melville, P. E. Repas, and J. M. Gray, "Properties and Control of Hot Rolled Steel," Journal of Metals, Vol. 20, pp 33, 1968.
3. Duckworth, W. E., "Metallurgy of Structural Steels: Present and Future Possibilities," Iron and Steel Institute Publication 104, pp 61, 1967.
4. Pickering F. B., "Precipitation of Intermetallic Compounds in Ferritic Steels," Iron and Steel Institute Publication 114, pp 131, 1969.
5. Larrabee, C. P., "Corrosion Resistance of HSLA Steels as Influenced by Composition and Environment," Corrosion, Vol. 9, pp 259, 1953.
6. Meyer, L., and D. Schawinhold, "Effects of Niobium on the Properties of Plain Carbon Weldable Steel," Stahl und Eisen, Vol. 87, pp 8, 1967.
7. Smith, R. P., "The Solubility of Niobium (Columbium) Carbide in Gamma Iron," Trans. AIME, Vol. 236, pp 220, 1966.
8. Smith, R. P., "The Solubility of Columbium Nitride in Gamma Iron," Trans. AIME, Vol. 224, pp 190, 1962.
9. Gray, J. M., D. Webster, and J. H. Woodhead, "Precipitation in Mild Steels Containing Small Additions of Niobium," Journal of the Iron and Steel Institute, Vol. 203, pp 812, 1965.
10. Gray, J. M., R. B. G. Yeo, P. E. Repas, and A. G. Melville, "Discussion Session III," Iron and Steel Institute Publication 104, pp 249, 1967.
11. de Kazinsky, F., A. Axnas, and P. Pachlaitner, "Some Properties of Niobium Treated Mild Steel," Jernkantorets Annaler, Vol. 147, pp. 408, 1963.
12. Gray, J. M., and R. B. G. Yeo, "Columbium Carbonitride Precipitation in Low Alloy Steels with Particular Emphasis on 'Precipitate-Row' Formation," Trans. ASM, Vol. 61, pp 255, 1968
13. Creswick, W. E., "Commercial Development of a Rimmed Low Alloy Precipitation Hardening High Strength Steel," Iron and Steel Institute Publication 104, pp 86, 1967.

14. Bungardt, K., K. Kind, and W. Oelsen, "The Solubility of Vanadium Carbide in Austenite," Archiv fur das Eisenhüttenwesen, Vol. 27, pp 61, 1956.
15. Narita, K., "Trace Elements in Steel: IV, Vanadium Nitride," Nippon Kapaki Sasshi, Vol. 78, No. 705, 1957.
16. Irvine, K. J., "The Development of High Strength Structural Steels," Iron and Steel Institute Publication 104, pp 1, 1967.
17. Stephenson, E. T., G. H. Karchner, and P. Stark, "Strengthening Mechanisms in Mn-V-N Steels," Trans. ASM, Vol. 57, pp 208, 1964.
18. Morrison, W. B., "The Influence of Small Niobium Additions on the Properties of Carbon-Manganese Steels," Journal of the Iron and Steel Institute, Vol. 201, pp 437, 1963.
19. Republic Steel Corporation, High Strength Low Alloy Steels, Cleveland, Ohio, 1968.
20. Irani, J. J., D. Dulieu, and G. Tither, "Role of Copper in Low Alloy Steels," Iron and Steel Institute Publication 114, pp 75, 1969.
21. Hall, E. O., "The Deformation and Aging of Mild Steel," Proceedings of the Physical Society, Vol. B64, pp 747, 1951.
22. Petch, N. J., "The Cleavage Strength of Polycrystals," Journal of the Iron and Steel Institute, Vol. 174, pp 25, 1953.
23. Pickering, F. B., and T. Gladman, "Metallurgical Developments in Carbon Steels," British Iron and Steel Research Association Report 81, pp 9, 1963.
24. Pickering, F. B., "Some Aspects of the Relationship Between Micro-structure and Mechanical Properties," Iron and Steel, Vol. 38, pp 110, 1965.
25. Jamieson, R. M., and J. W. Thomas, "Controlled Rolling of High Strength Skelp for the Manufacture of Large OD Pipe," Iron and Steel Institute Publication 104, pp 167, 1967.
26. Duckworth, W. E., and J. D. Baird, "Mild Steels," Journal of the Iron and Steel Institute, Vol. 207, pp 854, 1969.
27. Irvine, K. J., "Physical Metallurgy," Journal of the Iron and Steel Institute, Vol. 207, pp 837, 1969.
28. Korchynsky, M., Graham Research Laboratories, Jones and Laughlin Steel Corporation, Pittsburgh, Pennsylvania, personal communication to Dr. Clough.

29. Kouwenhoven, H. J., "The Influence of Ferrite Grain Size and Volume Fraction of Pearlite on the Lower Yield Stress and Luders Strain of Carbon Steel", Trans. ASM, Vol. 62, pp 437, 1969.
30. Morrison, W. B., "The Effect of Grain Size on the Stress-Strain Relationship in Low Carbon Steel," Trans. AMS, Vol. 59, pp 824, 1966.
31. Burns, K. W., and F. B. Pickering, "Deformation and Fracture of Ferrite-Pearlite Structures," Journal of the Iron and Steel Institute, Vol. 202, pp 899, 1967.
32. Allen, N. P., "Tensile and Impact Properties of High-Purity Iron-Carbon and Iron-Carbon-Manganese Alloys of Low Carbon Content," Journal of the Iron and Steel Institute, Vol. 174, pp 108, 1953.
33. Heslop, J. and N. J. Petch, "The Stress to Move a Free Dislocation in Alpha Iron," Philosophical Magazine, Vol. 1, pp 866, 1956
34. Irvine, K. J. and F. R. Pickering, "Low-Carbon Steels with Ferrite-Pearlite Structures," Journal of the Iron and Steel Institute, Vol. 201, pp 944, 1963.
35. MacDonald, J. K., Ship Structure Committee Report SSC-73, November, 1953.
36. Banta, H. M., R. H. Frazier, and C. H. Lorig, "Some Metallurgical Aspects of Ship Steel Quality," Welding Journal Research Supplement, Vol. 30, pp 79s, 1951.
37. De Kazinczy, F., and W. A. Backofen, "Influence of Hot Rolling Conditions on Brittle Fracture in Steel Plate," Trans. ASM, Vol. 53, pp 55, 1961.
38. Mackenzie, I. M., "Niobium Treated Carbon Steels," Journal of the West of Scotland Iron and Steel Institute, Vol. 60, pp 244, 1963.
39. Biggs, W. D., Brittle Fracture of Steel, Macdonald and Evans, London, 1960.
40. Petch, N. J., "The Ductile-Cleavage Transition in Alpha Iron," Fracture, John Wiley and Sons, New York, pp 54, 1959.
41. Rinebolt, J. A., and W. H. Harris, Jr., "Comparison of the Effects of Alloying Elements on the Lower and Upper Transition Temperatures," Trans. ASM, Vol. 44, pp 225, 1952.
42. Low, J. R., Jr., and M. Gensamer, "Aging and the Yield Point in Steel," Trans. AIME, Vol. 158, pp 207, 1944.
43. Tipper, C. F., "Effect of Direction of Rolling, Direction of Straining, and Aging on the Mechanical Properties of a Mild Steel Plate," Journal of the Iron and Steel Institute, Vol. 172, pp 143, 1952.

44. Garofalo, F., and G. V. Smith, "The Effect of Time and Temperature on Various Mechanical Properties During Strain Aging of Normalized Steel," Trans. ASM, Vol. 47, pp 957, 1955.
45. Gladman, T., B. Holmes, and F. B. Pickering, "Work Hardening of Low Carbon Steels," Journal of the Iron and Steel Institute, Vol. 208, pp 172, 1970.
46. Cryderman, R. L., A. P. Coldren, J. R. Bell, and J. D. Grozier, "Controlled-Cooled Structural Steels Modified with Columbium, Molybdenum, and Boron," Trans. ASM, Vol. 62, pp 561, 1969.
47. Ivanava, V. S., and L. K. Gordienko, New Ways of Increasing the Strength of Metals, Iron and Steel Institute Publication 109, 1968.
48. Koppenaal, T. J., "The Current Status of Thermomechanical Treatment in the Soviet Union," Trans. ASM, Vol. 62, pp 24, 1968.
49. Latham, D. J., "The Current Position of Thermomechanical Treatment Applied to Engineering and Tool Steels," Journal of the Iron and Steel Institute, Vol. 208, pp 50, 1970.
50. Irani, J. J., and D. J. Latham, "Applications of Isoforming and Applied Treatments to Low Alloy Steels," Iron and Steel Institute Publication 114, pp 55, 1969.
51. Underwood, E. E., Quantitative Stereology, Addison-Wesley Publishing Company, Reading, Massachusetts, 1970.
52. Dieter, G. E., Jr., Mechanical Metallurgy, McGraw-Hill Book Company New York, 1961.